
Project Title: Feasibility Studies on Process Coupling of Transesterification and Methanol Synthesis Using Cellulose and Bio-oil

Award Number: DE-EE0003156

Final Report

(July 1, 2010 – December 31, 2012)

Submitted to:

U. S. Department of Energy
National Energy Technology Laboratory

Submitted by:

Drs. Wei-Ping Pan and Yan Cao
Institute for Combustion Science and Environmental Technology
Western Kentucky University, Bowling Green, KY, 42101
Phone number: (270)792-3776 and (270)779-0202
Email: wei-ping.pan@wku.edu, and yan.cao@wku.edu

March15, 2013

DISCLAIMER

This report was prepared as an account of work sponsored by an agency of the United States Government. Neither the United States Government nor any agency thereof, nor any of their employees, makes any warranty, express or implied, or assumes any legal liability or responsibility for the accuracy, completeness, or usefulness of any information, apparatus, product, or process disclosed, or represents that its use would not infringe privately owned rights. Reference herein to any specific commercial product, process, or service by trade name, trademark, manufacturer, or otherwise does not necessarily constitute or imply its endorsement, recommendation, or favoring by the United States Government or any agency thereof. The views and opinions of authors expressed herein do not necessarily state or reflect those of the United States Government or any agency thereof.

TABLE OF CONTENTS

DISCLOSURE	2
TABLE OF CONTENTS	3
LIST OF FIGURES	4
LIST OF TABLES	6
1. Background	7
2. Executive Summary	14
3. Methods of Bio-diesel Characterizations.....	18
3.1 US and European Standards on Bio-diesel Quality	18
3.1.1 Reagents and Materials	18
3.1.2 Characterization of Bio-Diesel Using Standard Methods.....	20
3.2 Thermal Characteristics Methods	31
3.1.1 Reagents and Materials	31
3.1.2 Characterization of Bio-Diesel Using Thermal Characteristics Methods.....	31
4. Effects of Energy Input and Catalysts on Biodiesel Production	37
4.1 Effects of Ultrasonic Energy Input	38
4.1.1 Materials and Methods	38
4.1.2 Comparison of Conventional and Ultrasonication Methods	40
4.2 Effects of Heterogeneous Catalysts	44
4.2.1 Materials and Methods	44
4.2.2 Comparison of Conventional homogeneous and Heterogeneous Methods	45
5. Feasibility of Process Couplings	47
5.1 Process Basics.....	46
5.2 Setup of High-pressure Biodiesel Production Facility	48
5.3 Process Couplings	51
5.4 Final Solution on Process Couplings	57
6. Conclusion.....	59
7. Acknowledgement.....	60
8. References	61

LIST OF FIGURES

Figure 1. Overall scheme of triglyceride transesterification.....	19
Figure 2. Picture of the ambient pressure stirring reactor.....	19
Figure 3. Flow chart for biodiesel production	20
Figure 4. Picture of Varian 3800 GC.	23
Figure 5. Total Ion Chromatogram of standards and sample.	23
Figure 6. Calibration curves for methyl esters.....	25
Figure 7. Picture of Flash tester.....	26
Figure 8. Picture of viscometer	27
Figure 9. Picture of bomb calorimeter	29
Figure 10. The Picture of ICP-AES.	30
Figure 11. Overlay of TGA curves for biodiesel, commercial biodiesel and soybean oil under N2 flow.	33
Figure 12 OOT curves for biodiesel and commercial biodiesel.	34
Figure 13 OIT curves for biodiesel and commercial biodiesel.	34
Figure 14. Overlay of DSC curves for biodiesel and commercial biodiesel.	35
Figure 15. TGA curve for biodiesel under different humidity	36
Figure 16. Picture of Sonicator UPS 400	39
Figure 17. Calibration curve for internal standard-methyl undecanoate	40
Figure 18. Effect of stirring speed on biodiesel yield	42
Figure 19. Effect of reaction time on biodiesel yield.	42
Figure 20. Effect of amplitude on biodiesel yield	43
Figure 21. Effect of input energy on biodiesel yield	44
Figure 22. Schematic for experiment setup	45
Figure 23. Process concept	46
Figure 24. Bench scale stirring catalytic reactor system	48
Figure 25. The continuous-flow high pressure reactor	49
Figure 26. Overlay of TGA curves for samples 39, 41, commercial biodiesel and soybean oil ..	50
Figure 27. Overlay of sample 39, 41 and commercial biodiesel	54
Figure 28. Equilibrium conversion efficiency of methanol synthesis using syngas	56

LIST OF TABLES

Table 1. The detailed requirements of bio-diesel (B100)	21
Table 2: Composition of biodiesel samples based on EN 14103	22
Table 3. Summarized density results of samples	24
Table 4. Flash points for samples and commercial samples	24
Table 5. Clout point and pour points of biodiesel samples	27
Table 6. Summarized viscosity results of samples	27
Table 7. Summarized cetane number of samples	28
Table 8. Summarized acid number of samples	28
Table 9. Summarized iodine value of samples	29
Table 10. Summarized heating value of samples	30
Table 11. Summarized ICP results of samples	30
Table 12. Summarized GC result for the biodiesel	33
Table 13 Summarized TGA result for biodiesel and commercial biodiesel	33
Table 14 SA result for biodiesel adsorbing the water	35
Table 15. Biodiesel yield at different stirring speed	41
Table 16. Biodiesel yield at different time under same stirring speed	42
Table 17. Biodiesel production under different amplitudes	43
Table 18. Summarized ester content of the biodiesel under different catalysts	44
Table 19. Summarized biodiesel yield for different catalysts	46
Table 20. Bio-diesel production under supercritical conditions	51
Table 21. Summary of Qualities of Produced Bio-diesel under supercritical methanol conditions	53
Table 22. Syngas-direct bio-oil transesterification	55

1. Background

Petroleum-based liquid hydrocarbons is exclusively major energy source in the transportation sector. Thus, it is the major CO₂ source which is associated with greenhouse effect. In the United States alone, petroleum consumption in the transportation sector approaches 13.8 million barrels per day (Mbbl/d)¹. It is corresponding to a release of 0.53 gigatons of carbon per year (GtC/yr)², which accounts for approximate 7.6 % of the current global release of CO₂ from all of the fossil fuel usage (7 GtC/yr)³. For the long term, the conventional petroleum production is predicted to peak in as little as the next 10 years to as high as the next 50 years⁴⁻⁵. Negative environmental consequences, the frequently roaring petroleum prices, increasing petroleum utilization and concerns about competitive supplies of petroleum have driven dramatic interest in producing alternative transportation fuels, such as electricity-based⁶, hydrogen-based⁷ and bio-based transportation alternative fuels.

Use of either of electricity-based or hydrogen-based alternative energy in the transportation sector is currently laden with technical and economical challenges. The current energy density of commercial batteries is 175 Wh/kg of battery⁸. At a storage pressure of 680 atm, the lower heating value (LHV) of H₂ is 1.32 kWh/liter. In contrast, the corresponding energy density for gasoline can reach as high as 8.88 kWh/liter. Furthermore, the convenience of using a liquid hydrocarbon fuel through the existing infrastructures is a big deterrent to replacement by both batteries and hydrogen. Biomass-derived ethanol and bio-diesel (biofuels) can be two promising and predominant U.S. alternative transportation fuels. Both their energy densities and physical properties are comparable to their relatives of petroleum-based gasoline and diesel, however, biofuels are significantly environmental-benign.

Ethanol can be made from the sugar-based or starch-based biomass materials, which is easily fermented to create ethanol. In the United States almost all starch ethanol is mainly manufactured from corn grains. The technology for manufacturing corn ethanol can be considered mature as of the late 1980s. In 2005, 14.3 % of the U.S. corn harvest was processed to produce 1.48×10^{10} liters of ethanol⁹, energetically equivalent to 1.72 % of U.S. gasoline usage¹⁰. Soybean oil is

Novel Oxygen Carriers for Coal-fueled Chemical Looping

extracted from 1.5 % of the U.S. soybean harvest to produce 2.56×10^8 liters of bio-diesel⁹⁻¹⁰, which was 0.09 % of U.S. diesel usage¹⁰. However, reaching maximum rates of bio-fuel supply from corn and soybeans is unlikely because these crops are presently major contributors to human food supplies through livestock feed and direct consumption. Moreover, there currently arguments on that the conversion of many types of many natural landscapes to grow corn for feedstock is likely to create substantial carbon emissions that will exacerbate globe warming¹¹⁻¹². On the other hand, there is a large underutilized resource of cellulose biomass from trees, grasses, and nonedible parts of crops that could serve as a feedstock¹³. One of the potentially significant new bio-fuels is so called “cellulosic ethanol”, which is dependent on break-down by microbes or enzymes. Because of technological limitations (the wider variety of molecular structures in cellulose and hemicellulose requires a wider variety of microorganisms to break them down) and other cost hurdles (such as lower kinetics), cellulosic ethanol can currently remain in lab scales¹⁴. Considering farm yields, commodity and fuel prices, farm energy and agrichemical inputs, production plant efficiencies, byproduct production, greenhouse gas (GHG) emissions, and other environmental effects, a life-cycle evaluation of competitive indicated that corn ethanol yields 25 % more energy than the energy invested in its production, whereas soybean bio-diesel yields 93 % more¹⁵. Relative to the fossil fuels they displace, greenhouse gas emissions are reduced 12 % by the production and combustion of ethanol and 41 % by bio-diesel. Bio-diesel also releases less air pollutants per net energy gain than ethanol.

Bio-diesel has advantages over ethanol due to its lower agricultural inputs and more efficient conversion. Thus, to be a viable alternative, a bio-fuel firstly should be producible in large quantities without reducing food supplies. In this aspect, larger quantity supplies of cellulose biomass are likely viable alternatives. U. S. Congress has introduced an initiative and subsequently rolled into the basic energy package, which encourages the production of fuel from purely renewable resources, biomass¹⁶. Secondly, a bio-fuel should also provide a net energy gain, have environmental benefits and be economically competitive. In this aspect, bio-diesel has advantages over ethanol. The commonwealth of Kentucky is fortunate to have a diverse and

Novel Oxygen Carriers for Coal-fueled Chemical Looping

abundant supply of renewable energy resources. Both Kentucky Governor Beshear in the energy plan for Kentucky “Intelligent Energy Choices for Kentucky’s Future”¹⁷, and Kentucky Renewable Energy Consortium¹⁸, outlined strategies on developing energy in renewable, sustainable and efficient ways. Smart utilization of diversified renewable energy resources using advanced technologies developed by Kentucky public universities, and promotion of these technologies to the market place by collaboration between universities and private industry, are specially encouraged. Thus, the initially question answering Governor’s strategic plan is if there is any economical way to make utilization of larger quantities of cellulose and hemicellulose for production of bio-fuels, especially bio-diesel.

There are some possible options of commercially available technologies to convert cellulose based biomass energy to bio-fuels. Cellulose based biomass can be firstly gasified to obtain synthesis gas (a mixture of CO and H₂), which is followed up by being converted into liquid hydrocarbon fuels or oxygenate hydrocarbon fuel through Fischer-Tropsch (F-T) synthesis. Methanol production is regarded to be the most economic starting step in many-year practices of the development of F-T synthesis technology since only C₁ synthesis through F-T process can potentially achieve 100% conversion efficiency. Mobil’s F-T synthesis process is based on this understanding. Considering the economical advantages of bio-diesel production over ethanol and necessary supply of methanol during bio-diesel production, a new opportunity for bio-diesel production with total supplies of biomass-based raw materials through more economic reaction pathways is likely identified in this proposal. The bio-oil part of biomass can be transesterified under available methanol (or mixed alcohols), which can be synthesized in the most easy part of F-T synthesis process using synthesis gas from gasification of cellulose fractions of biomass. We propose a novel concept to make sense of bio-diesel production economically though a coupling reaction of bio-oil transesterification and methanol synthesis. It will overcome problems of current bio-diesel producing process based on separated handling of methanol and bio-oil.

Drawbacks of Conventional Bio-diesel Process and Opportunity. The bio-oils can be,, but can not be directly, used as engine fuels since it has lower cetane index, higher flash point, coking

Novel Oxygen Carriers for Coal-fueled Chemical Looping

during burning and instability. Most importantly, they are either extremely viscous (vegetable oils) or become solid at room temperature (animal fat). Viscosities of vegetable oils range from 10 to 20 times greater than that of petroleum diesel fuel¹⁹. Viscosity is the most important property of bio-diesel since the high viscosity means that handling of fuel injection is difficult, particularly at low temperatures. The transesterification process of vegetable oils and animal fats are the most common methods to control viscosities of these raw bio-oils. Transesterification is the process of using a monohydric alcohol in the presence of a most likely alkali catalyst (hydroxides of alkali metals) to chemically break the raw bio-oil molecules into esters (bio-diesel) with glycerol as a byproduct²⁰. The produced bio-diesel has a viscosity and a flash point close to those of petroleum diesel fuels. Therefore, it can be burned directly in unmodified diesel engines with very low deposit formation. Methanol and ethanol are most frequently used monohydric alcohol in transesterification process to produce methyl or ethyl esters. Ethanol is generally a preferred alcohol in the transesterification process compared to methanol because it can be derived from agricultural products and is renewable and biologically less objectionable in the environment. However, methanol is lower in cost and has physical and chemical advantages (polar and shortest chain alcohol). Furthermore, much less reaction time is required for methanol transesterification with similar yields of esters. Methyl esters also have several other outstanding advantages among other renewable and clean engine fuel alternatives¹⁹.

However, there are still several drawbacks of conventional methanol based transesterification process. 1) It often takes at least several hours to ensure the transesterification reaction is complete, even under assist of alkali catalyst. This low conversion kinetics make the transesterification process difficult to scale-up. 2) Removal of added catalysts is technically difficult and brings extra cost to the final product²¹. 3) Transesterification process can not effectively convert free fatty acids to methyl esters, which decrease production of bio-diesel. Additionally, more catalyst is required to neutralize free fatty acids of a bio-oil with higher free fatty acids content. This not only causes the production process to be longer and more complexity. Generally refined vegetable oils with free fatty acids content of less than 0.5%

Novel Oxygen Carriers for Coal-fueled Chemical Looping

should be used in the conventional transesterification process²⁴. 4) It is well known that the vegetable oils/fats used as a raw material for the transesterification should be water-free since the presence of water has negative effects on the reaction²³. Water can consume the catalyst and reduce catalyst efficiency. The presence of water even has a greater negative effect than that of the free fatty acids. So, the water content should be kept below 0.06%²⁴ by the conventional process. These problems may hinder the most efficient utilization of crude bio-oils since they generally contain water and free fatty acids.

Most recently, a few studies have been conducted via non-catalytic transesterification with supercritical methanol (250–400 K and 15–35 MPa)^{25–31}. Compared with conventional catalytic processes under barometric pressure, the supercritical methanol process is non-catalytic, is much simpler to purify the products, has improved reaction kinetics, is more environmentally friendly and is lower in energy use. There are several other advantages of supercritical methanol transesterification over the conventional transesterification process. 1) Supercritical methanol has a high potential for both transesterification of triglycerides and methyl esterification of free fatty acids to methyl esters; and 2) the presence of water positively affected the formation of methyl esters in the supercritical methanol method²⁸, which is much different from water's function in the traditional transesterification process. However, it was reported that transesterification process under such high pressures (supercritical conditions of water) would be not an economic alternative due to its high operating costs³².

Drawbacks of Conventional Methanol Synthesis and Opportunity. Methanol was firstly produced by “wood distillation”, which is a pyrolysis process with low yields and intensive feed-stock handling. Its first commercialization began in 1923 by BASF using ZnO–Cr₂O₃ catalyst under 350–400 °C and 24–30 MPa. Numerous improvements have been pursued to reduce investment costs. The robust indicator for cost reduction is the minimization of energy transfer duty within each sub-division of the whole process³³. Reactions are exothermic and result in a reduction in volume. The conversion reactions are, therefore, thermodynamically favored by low temperatures and high pressures. Low pressure operation is presently favored in

Novel Oxygen Carriers for Coal-fueled Chemical Looping

methanol synthesis due to its low cost. But, it tends to result in a low fraction of the synthesis gas being converted in each pass (typically about 10 % conversion efficiency). Therefore, the processes need to use a recycle loop to achieve adequate yields, with a purge gas to remove impurities that would otherwise build up over time. On the other hand, stronger exothermic property of methanol synthesis reaction consequently requires significant cooling duty. The resulting recycle and cooling duty are largely responsible for the investment cost of methanol synthesis process. In the 1960s, a major improvement was achieved by using the high activity Cu/ZnO catalyst to bring down operational temperature and pressure to be namely 250–280 °C and 6–8 MPa. These improvements resulted in reductions of both the compression and heat exchange duty in the recycle loop (5-10 %). The consumption of synthesis gas was also reduced by a few percentages; however, the cooling duty is still a big hurdle for the economics of the methanol synthesis process.

More recently, various schemes for once-through operation have been conceived to avoid the large gas recycle. Some once-through schemes were based on multiple reactors placed in series with inter-stage removal of methanol, e.g. by means of condensation³⁴, by absorption in a liquid³⁵ or by reactive chromatography³⁶. Other once-through schemes attempted to remove the methanol inside the synthesis reactor, e.g. by means of a methanol permeating membrane³⁷, by means of a trickling liquid absorbent or trickling solid adsorbent particles³⁸⁻³⁹. Soon it was realized that most of these once-through schemes substitute the large energy duty of the gas recycle loop by other large transfer duties. For example, the series condensation scheme requires extensive inter-stage cooling. The use of solid adsorbent^{35,38} and liquid absorbent³⁹ require regeneration of the adsorbent/absorbent. Reactive chromatography³⁶ requires important energy transfer duty in the sweep gas line. Thus, one could reasonably expect that such substitutions of energy transfer duties likely have a limited economic potential. The in-situ removal of methanol by means of a selective membrane likely implies a smaller heat transfer duty, however, is will be expected to be fairly expensive on a large scale. The economics of the methanol synthesis process is also closely related to synthesis gas production. Significant cost reduction has been

Novel Oxygen Carriers for Coal-fueled Chemical Looping

claimed for combinations of steam reforming and partial oxidation of methane⁴⁰. If synthesis gas (CO and H₂) is used, the ideal ratio of H₂ and CO in synthesis gas of 2, promised significant reductions in heat transfer duty and in investment cost⁴¹⁻⁴³. Alternative reaction routines for methanol production are using CO₂ to replace CO in feedstock stream⁴⁴. Process product of CO₂ from synthesis gas production using cellulose biomass feedstock including the mediate product (such as glycerol) from methanol synthesis, could be candidate feedstock.

The overall goal of this project is to demonstrate the feasibility of in-site coupling concept on bio-diesel production using both bio-oil fractions of biomass and synthesis gas from various cellulose fractions of biomass, as well as instant separation of process product. The specific goals of the proposed process is the investigation of compatibility of these two reactions within single reactor and associated process heat transfer, thermodynamics equilibrium shift, improved reaction conversion kinetics and yields, as well as process product separation.

2. Executive Summary

The Sponsored Programs of WKU is the compliance management for the entire campus. They are responsible for both the fiscal compliance, in addition to the coordination and implementation of pre and post-award documentation. Dr. Wei-Ping Pan is the Principal Investigator of the project, and is responsible for the carrying out of the objectives outlined in this proposal. Dr. Yan Cao, serve as the Co-Principal Investigator, who is responsible for directing the team in carrying out the objectives outlined.

This project investigates feasibilities of combining the transesterification bio-diesel production into the traditional methanol production process. In this process, the raw materials for process feedstock will be completely the biomass, include cellulose fractions of biomass and bio-oil fractions of biomass. The process product will be either the bio-diesel or mixed bio-diesel and bio-methanol, which both can be directly fed as the alterative liquid fuel and also has some improvement on fuel handling³⁹. Since its capability of the complete utilization of every part of biomass (both cellulose biomass and bio-oils) and capability of the in-site optimization of reaction heat transfer and thermodynamics equilibrium shift and instant separation of process product, the proposed process can better balance several drawbacks of individual process during production of bio-diesel. This is a totally “green” process with almost all aspects of process to embody the characterization of renewable, compatibility and economic.

Major achievements in this stage include:

1) Approach I, identification major issues and setup all necessary supporting works, such as setup test procedures to test quality index of bio-diesel products, setup critical parameters, capacity and capability of test facility, and identification and characterization of targeted opportunity bio-oil resources which will be used in this test.

The conventional transesterification method for producing biodiesel and the methods for evaluating the biodiesel quality to meet the requirements of ASTM D 6751 or EN 14214 standards were setup. The quality of biodiesel includes physical characterization such as, density, viscosity, flash point, cloud point, pour point, acid number, and iodine value, and chemical characterization, such as ester content, free glycerin and total glycerin. This QA/QC platform was used throughout this project for sample analysis and provides guidelines on conversion efficiencies of process and product quality from our reactors.

Novel Oxygen Carriers for Coal-fueled Chemical Looping

Thermal analysis is an efficient tool for measuring properties, such as crystallization temperature, and thermal and oxidative stabilities. The thermal behaviors of biodiesel at low and high temperatures were investigated by using thermogravimetric analyzer, differential scanning calorimetry, pressurized differential scanning calorimetry (PDSC), and sorption analyzer (SA). The constituents of the soy biodiesel as determined by gas chromatography show that methyl esters content was 99 % and of these 84 % were unsaturated fatty acids. TG results illustrate that the total weight loss of the biodiesel was 99 % below 300 °C under nitrogen flow, indicating a high purity biodiesel. The onset decomposition temperature and the peak temperature of the soy biodiesel were 193 °C and 225 °C, respectively, implying the biodiesel has good thermal stability. PDSC results show that the oxidation onset temperature of the soy biodiesel was 152 °C, and the oxidative induction time was 24 min. DSC results demonstrate that the onset crystallization temperature of the soy biodiesel was 1.0 °C. The SA results point out that with increasing temperature and humidity, the soy biodiesel absorbed more water, and in which humidity was the dominant factor. The water absorption and desorption of the soy biodiesel is a non-reversible process. The preferable storage conditions for soy biodiesel occur when humidity is less than 30 % and the temperature is less than 30 °C. Thermal analysis was found to be faster alternative methods for thermal behavior studies as compared with conventional standard methods.

The synthesis of biodiesel from soybean oil under ultrasonication as well as the conventional method, using homogeneous alkali catalysis were studied and compared. Compared with the conventional method of mechanical stirring, the ultrasonication method was an efficient method for biodiesel synthesis. The biodiesel yields dramatically increased to 90 % in 5 minutes while in the conventional method, the biodiesel yields was 80 % in 15 minutes, indicating that the ultrasonication energy input significantly breakthrough the mass transfer limitation between methanol and bio-oil. SrO, CaO and γ -Al₂O₃ were also chosen as the heterogeneous catalysts for the biodiesel synthesis, indicating the efficiencies of heterogeneous catalysts on transesterification. Tests also indicated SrO had the highest efficiency for bio-oil transesterification.

2) Approach II, Technical development of coupling concept and investigation of thermodynamics, kinetics and energy balance, product selectivity, productivity.

The background of process design is based on the process analysis of the methanol synthesis

Novel Oxygen Carriers for Coal-fueled Chemical Looping

process, which is highlighted by the importance, feasibilities and potentials in aspects of heat management, thermodynamic shift on one-pass conversion efficiency and synthesis gas stoichiometry. Both the effective in-situ removal of methanol and the economic supply of synthesis gas with the optimized ratio of H₂/CO are likely two major steps to control the large heat transfer duty and further reduce costs for methanol synthesis. The economic index could be further improved if the generated heat in the exothermic methanol synthesis can be taken in-site with coupling other endothermic reactions simultaneously. In an optimal situation, these coupling reactions could be compatible in the in-site integration of both heat transfer and thermodynamic equilibrium shift by methanol removal. The removal of methanol in methanol synthesis could also be realized by consumption of generated methanol by the bio-oil transesterification. To ensure the catalysts are active and process economically, the coupling process is operated at medium temperature and pressure ranges, such as 200–300 °C and 6-10 MPa. These temperature and pressure ranges could be perfectly compatible to supercritical CO₂ condition, which are different from current supercritical water conditions. CO₂ is used as a reaction-assisting solvent and process product separation agent by its unique properties under its supercritical CO₂ conditions (gaseous and aqueous status). CO₂ supply will be directly supplied from process products. In order to prepare a genuine bio-diesel, it is essential to use methanol prepared from cellulose biomass but not natural gas for bio-diesel production. The raw feedstock for synthesis gas production using co-gasification technologies will be cellulose biomass, together with any byproducts from bio-diesel production process.

3) Approach III. Process integration and demonstration, including Setup of fully-functioned lab-scale facility assembles, demonstration of coupling concept in this facility, build-up necessary parameters for system scale-up; Conclusion on feasibility of concept on process coupling and integration, and suggestion on alternative routines to overcome technical hurdles during process coupling; Build-up economical factors of coupling process, compared to the conventional bio-diesel production, in view of process economics and efficiency.

Two fully-functional high pressure systems have been built, including 1) a bench top stirring-type liquid catalytic reactor, in which important parameters on methanol transesterification reactions under higher pressure and temperatures were obtained. Tests indicated that the optimal conditions of methanol transesterification reactions were temperature dependent, not pressure dependent. Tests also indicated that the direct feeding of cellulosic

Novel Oxygen Carriers for Coal-fueled Chemical Looping

biomass was infeasible to synthesize bio-diesel and cellulosic biomass gasification need to be excluded from the proposed integration process; 2) continuous-flow syngas high pressure catalytic reactor, in which the feasibility of direct feeding syngas into the transesterification for bio-diesel production was confirmed using commercially-available methanol catalyst.

A previously proposed process regarding the direct feeding of cellulosic biomass was confirmed to be infeasible, because an existing technical conflicts in optimal operational conditions between the syngas production using cellulosic biomass and transesterification of bio-oil. However, a modified process starting with a syngas feeding into the transesterification of bio-oil, which excluded the biomass gasification, was successfully accomplished for bio-diesel production. The catalyst used in this modified process was from a commercial supply, which was original for production of methanol. A methanol catalyst was presented effective for transesterification of bio-oil. The optimal conditions for this new process were temperature dependent, not pressure dependent, although a higher pressure was preferable for methanol synthesis in view of thermodynamics. This was because methanol was only an intermediate product, and thus was not required in a higher concentration which was limited by thermodynamics of the syngas-to-methanol reaction. Overall, the gasification of cellulosic biomass should be excluded from the previously proposed integrated process, and a separately operated gasification of biomass-derived syngas should be on line.

The accomplishment of the modified process was in its instant integration of commercially-available refinery process, which is cost effective for the bio-diesel production. The accomplishment was also extended to the confirmation of the effectiveness of commercial methanol catalysts on both the methanol synthesis and the followed-up methanol transesterification of bio-oil to produce the bio-diesel. Combining both of two unique accomplishments, cost reductions based on this new bio-refinery process, using available commercial facility to produce the bio-diesel, could be expected. The most likely commercial process which could be used for this process would be the inexpensive methanol synthesis facility and process.

3. Methods of Bio-diesel Characterization

There are two standards for quality control of bio-diesel, which are ASTM D 6751 and EN 14214. These two standards require measurements of multiply parameters of bio-diesel for QA/QC purpose. Previous research shows that thermal analysis is an effect technique for evaluating the characteristics of the biodiesel, such as thermal and oxidative stability, phase transitions and water absorbing ability⁴⁵⁻⁵¹. It's a faster alternative for thermal behavior studies since by the standard method for such determinations the major drawback is time of analysis. Moreover, only a small amount of samples was needed. As a result, thermal analysis is widely used on evaluating the thermal behavior of the biodiesel. Teixeira et al studied the cloud and pour points of the biodiesel using DSC⁴⁶. Castello et al found that thermogravimetry is a good technique for determining the water content in the glycerol⁴⁷. Conceicao et al investigated the thermal stability and oxidative degradation of biodiesel by using SDT and DSC⁴⁸⁻⁵¹. So in the first quarter, the biodiesel was produced through the conventional transesterification method and the thermal behaviors of biodiesel were characterized using TGA, DSC, PDSC and SA.

The setup of these standards was introduced in this chapter, together with the development of some simple and quick methods for bio-diesel characterization. For comparison purpose, the conventional liquid catalysts was firstly used in the synthesis of bio-diesel in this chapter.

3.1. US and European Standards on Bio-diesel Quality

3.1.1 Reagents and Materials.

Commercial edible grade soybean oil was obtained from Walmart. Methanol (99.9%) was obtained from Fisher Scientific (Pittsburgh, USA). Potassium hydroxide pellets and biodiesel standards, such as linoleic acid methyl ester, palmitic acid methyl ester, oleic acid methyl ester, linolenic acid methyl ester, stearic acid methyl ester, heptadecanoic acid methyl ester, glycerin, monoolein, diolein, triolein, butanetriol and tricaprin were purchased from Sigma-Aldrich, Inc. (St. Louis, USA). All the chemicals are analytical grade.

The most commonly used method for producing biodiesel is transesterification of triglycerides or fatty acids with an alcohol in the presence of a strong catalyst (acid, base or enzyme) producing a mixture of fatty acid alkyl esters and glycerol (Fig 1). Conventional transesterification reaction was carried out in a 2000 mL glass reactor with a condenser (Fig 2). The mechanical stirrer speed was 100~600 rpm. Heating was achieved by means of a water bath. The amount of methanol,

Novel Oxygen Carriers for Coal-fueled Chemical Looping

soybean oil and potassium hydroxide used in the reactions were calculated based on their molar concentration to give 200 g of reaction mixture. The reaction procedure was as follows: First, an amount of soybean oil was heated in an oven up to 110 °C for 1 h, and then added into the glass reactor. After the temperature increased to 65 °C, the mixture of KOH dissolved in methanol was added. The stirrer speed was 400 rpm. After reacting for 1 hour, the mixture was transferred to a separating funnel and settled overnight. The upper layer was the mixture of coarse biodiesel with catalysts and methanol, while the lower layer was a mixture of glycerol and methanol. The upper layer was first vacuum distilled at 80 °C to recover the methanol, then washed with hot water (50 °C) until the pH was 7, and then dried with anhydrous sodium sulfate, as shown in Figure 3.

Figure 1. Overall scheme of triglyceride transesterification

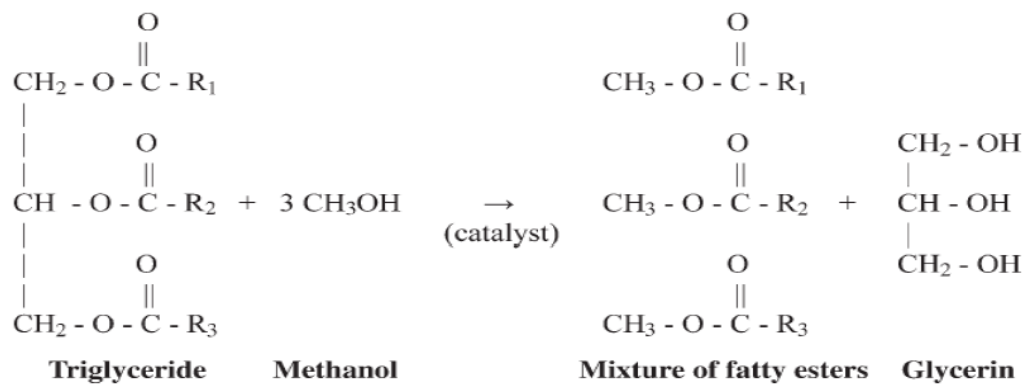
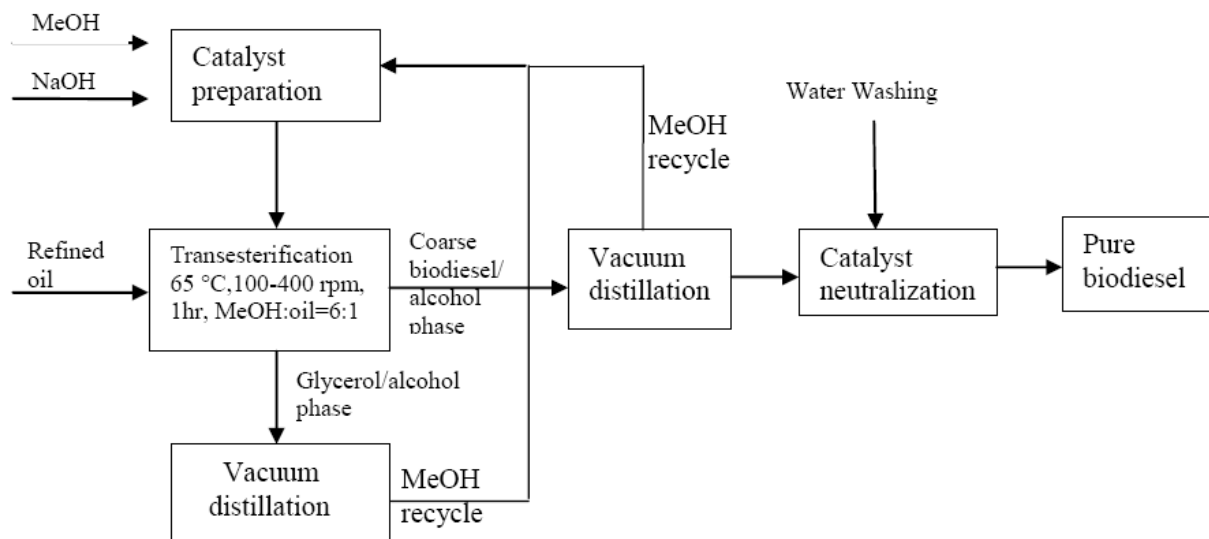


Figure 2. Picture of the ambient pressure stirring reactor



Novel Oxygen Carriers for Coal-fueled Chemical Looping

Figure 3. Flow chart for biodiesel production



3.1.2 Characterization of Bio-Diesel Using Standards

The properties of methyl esters were determined using ASTM methods or British standard methods (Table 1). The flash point was determined by a Pensky–Martens closed-cup flash tester (Fisher, USA), according to ASTM D 93. Cloud point and pour point determinations were made using ASTM D2500 and ASTM D97, respectively. The kinematic viscosities were determined at 40 °C using a CFR-075 glass capillary viscometer (Ramin Co, USA) according to ASTM D445. The densities were determined by hydrometer (Hydrometer set 100, Fisher, USA) using ASTM D1298. Distillation characteristics were studied by distillation apparatus, following ASTM D86. The sulfur content was measured according to ASTM D129. Ash content was determined according to ASTM D482. The water contents were determined following ASTM D95. The acid number and iodine value of the biodiesel were titrated following ASTM D974 and EN3961, respectively. The cetane value was calculated according to ASTM D976. Heating value was determined using a Leco AC700 bomb calorimeter following ASTM D2015. The K⁺, Ca²⁺, Mg²⁺ and P contents were determined using ICP-AES.

The physicochemical characteristics of petroleum diesel were determined from a commercial diesel while the results of commercial biodiesel and samples 1~4 were measured based on ASTM methods or EN methods.

Table 1 Detailed requirements for biodiesel (B100)

Property	ASTM D 6751		EN 14214	
	Test method	Limits	Test method	Limits
Calcium & magnesium,	EN14538	5 ppm max	EN14538	5 ppm max
Ester content	-	-	EN14103	96.5% (m. m ⁻¹) min
Linolenic acid content	-	-	EN14103	12.0% (m. m ⁻¹) max
Free glycerine	ASTM D 6584	0.02%(w/w) max	EN14105	0.02% (m. m ⁻¹) max
Total glycerine	ASTM D 6584	0.24% (w/w) max	EN14105	0.25% (m m ⁻¹) max
Water and sediment	ASTM D 2709	0.05 % volume		
Specific gravity at 15°C	ASTM D 1298	--	EN ISO 3675	0.86-0.9
Flash point	ASTM D 93	93 °C min	EN ISO 3679	120 °C min
Pour point	ASTM D 2500	Not specified	-	-
Cloud point	ASTM D 97	Not specified	-	-
Viscosity at 40°C	ASTM D 445	1.9-6.0 mm ² s ⁻¹	EN ISO 3104	3.5-5 mm ² s ⁻¹
Acid number (mg KOH. g ⁻¹)	ASTM D 974	<0.05% (w/w)max	EN ISO 20864	10.0 mg.kg ⁻¹ max
Iodine value (g I ₂ 100g ⁻¹)	-	-	EN ISO 3916	120 I ₂ .100g ⁻¹ max
Sulfur (mass %)	ASTM D129	Max.0.05%	EN ISO 20884	10 ppm
Cetane number	ASTM D976	47 min	EN ISO 5165	51 min
Phosphorus content	ASTM D 4951	0.001%max	EN 14107	10 mg kg ⁻¹ max
Gross Heating value cal g ⁻¹)	ASTM D2015	-	--	--

Ester content. The ester content refers to the percentage of methyl esters of fatty acids present in the sample, which is measured by gas chromatography. Based on EN 14103, the ester content is calculated using the internal standard method and the fatty acid methyl ester (FAME) content should be more than 96% while the linolenic acid methyl ester content should be between 1% and 15%.

The FAME composition was analyzed by a Varian 3800 gas chromatograph (Fig 4) fitted with a polar capillary column (Wax 30 m×0.25 mm×0.25 μm, Restek, USA) and a flame ionization detector (GC-FID). The temperature program was as follows: The initial oven temperature was 190 °C, ramping to 200 °C at the rate of 0.5 °C min⁻¹, isothermal for 20 min, and then ramping to 240 °C min⁻¹ at the rate of 20°C min⁻¹, isothermal for 2 min. The injector and detector temperatures were 220 °C and 230 °C respectively. The split ratio was 50. The sample was diluted and injected with a volume of 1.0μL. The total ion chromatograph of the biodiesel and the standard is shown in Figure 5. It can be seen that the methyl esters can be clearly separated. The retention times for methyl palmitate, methyl stearate, methyl oleate, methyl linoleate and methyl linolenate are 6.59, 11.04, 11.71, 13.29 and 15.41 min, respectively. The external standard method was used in the present study to calculate the ester content of the

Novel Oxygen Carriers for Coal-fueled Chemical Looping

biodiesel. The calibration curves for methyl palmitate, methyl stearate, methyl oleate, methyl linoleate and methyl linolenate are shown in Figure 6.

The ester content of the biodiesel samples was about 95% while the ester content of sample 4 was 84.9%, indicating that a higher ratio of methanol to oil did not increase the biodiesel yield. A methanol to oil ratio of 6:1 or 7:1 may be the best for high biodiesel yield. It also can be seen that the stirring speed did not influence the biodiesel yield if the reaction time was long enough. The ester content of commercial biodiesel was also measured and the ester content was 98.9%. Results showed that high catalyst content not only influenced the biodiesel content but also accelerated the saponification when washing with the hot water. During the purification of biodiesel process, the volume of water for washing biodiesel was nearly 5 times that of the biodiesel. So separation of a large amount of wastewater, cleaning the catalyst and the products are problems in the conventional method. So developing a solid catalyst is an urgent issue.

Table 2: Composition of biodiesel samples based on EN 14103

Sample ID	Experiment condition	Methyl Palmitate (16:0)	Methyl Stearate (18:0)	Methyl oleate (18:1)	Methyl Linoleate (18:2)	Methyl linolenate (18:3)	Methyl ester content (%)
Sample 1	Methanol: oil=6:1 Stirring speed: 100 rpm Catalyst: 2 wt % T: 65°C, Time: 60 min	9.9	4.4	22.1	51.6	6.7	94.8
Sample 2	Methanol: oil=6:1 Catalyst: 0.5 wt % Stirring speed: 400 rpm T: 65°C, Time: 60 min	9.8	4.5	21.8	54.2	7.9	98.2
Sample 3	Methanol: oil=7:1 Catalyst: 0.5 wt % Stirring speed: 400 rpm T: 65°C, Time: 60 min	9.5	4.3	21.3	52.1	7.9	95.1
Sample 4	Methanol: oil=12:1 Catalyst: 0.5 wt % Stirring speed: 400 rpm T: 65°C, Time: 60 min	9.5	4.3	11.3	52.8	7.0	84.9
Commercial Biodiesel	--	10.1	4.7	20.9	54.5	8.8	98.9

Free and Total Glycerin. Glycerin content is an indicator of the quality of biodiesel, which can be in the form of free glycerin or bond glycerin in the form of glycerides. The bonded glycerin is the glycerin portion of mono-, di-, and triglyceride molecules, which is the un-reacted or partially reacted forms of triglyceride. A high content of glycerin can lead to build up in

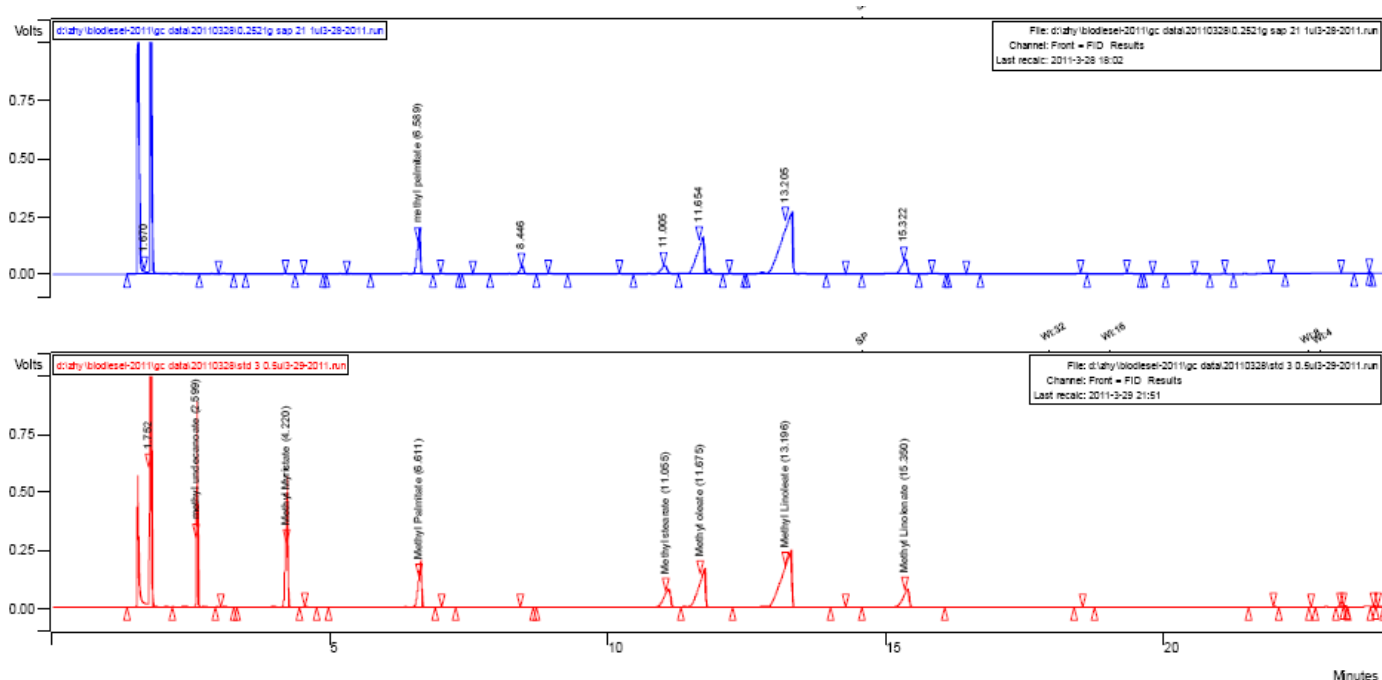
Novel Oxygen Carriers for Coal-fueled Chemical Looping

fueling systems, clogged fuel systems, injector fouling, filter plugging and valve deposits⁴⁹. The glycerin content was determined based on ASTM D6584 using a Varian GC CP 3800 with an FID detector. The system is still being set up.

Figure 4. Picture of Varian 3800 GC.



Figure 5. Total Ion Chromatogram of standards and sample.



Novel Oxygen Carriers for Coal-fueled Chemical Looping

Density. Density is an important parameter for the biodiesel, which was measured using ASTM D1298. The density of biodiesel was determined using a hydrometer (Fisher, USA). Based on EN 14214 method, the density of biodiesel is 0.86~0.90 g.cm⁻³, which is higher than that of petroleum diesel. The density of biodiesel samples was within the limits (Table 3). Tests have shown that lower density will promote the smaller size of droplets on injection of the fuel in the combustion chamber, which leads to better combustion and lower particles emission

Flash point. The flash point is the lowest temperature at which the sample can vaporize to form an ignitable mixture in air, which is important to fuel handling and storage. According to ASTM D93, the minimum flash point of biodiesel is 93 °C using the closed cup. The flash point of biodiesel was measured by Pensky-Martens closed cup flash tester (Fig 7). N-decane and n-hexadecane were used for calibrating the temperature. From Table 4, it can be seen that the flash point of all the biodiesel samples were in the limits and the flash point of biodiesel was higher than that of petroleum diesel, which is better for storage and transportation.

Table 3: Summarized density results for samples.

Sample ID	Petroleum diesel	Commercial biodiesel	Sample 1	Sample 2	Sample 3
Density (g.cm ⁻³)	0.82~0.86	0.88	0.87	0.88	0.86

Table 4 Flash point for samples and commercial biodiesel

Sample ID	Petroleum diesel	Commercial biodiesel	Sample 1	Sample 2	Sample 3
Flash point (°C)	60	118	120	97	115

Novel Oxygen Carriers for Coal-fueled Chemical Looping

Figure 6: Calibration curves for methyl esters.

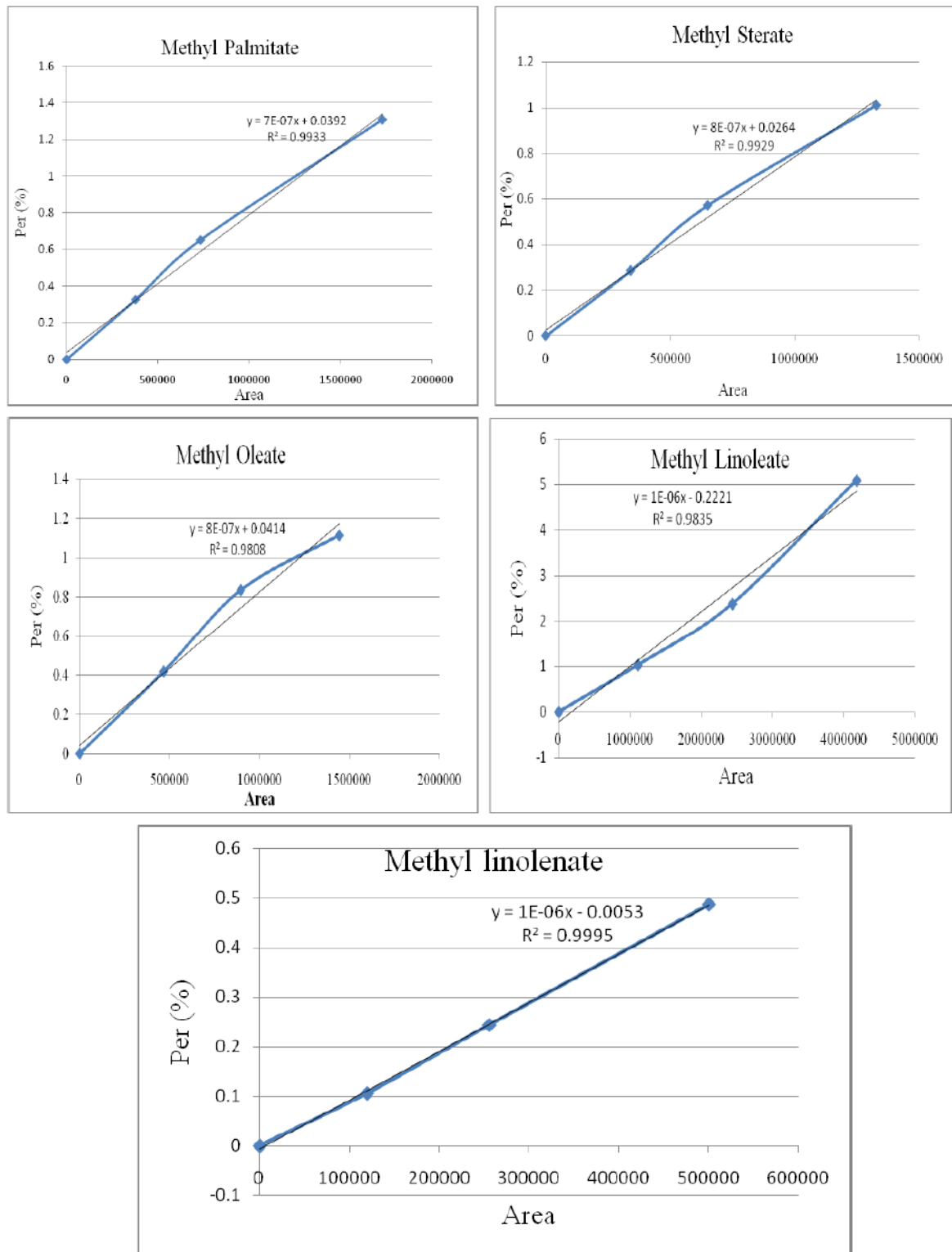


Figure 7. Picture of Flash tester



Cloud point and pour point. Cold flow properties of biodiesel are important indicators of the applicability of the biodiesel. The key flow properties are cloud point and pour point. Cloud point is the lowest temperature at which wax crystals begin to form in the fuel under prescribed conditions while the pour point is the lowest temperature at which the biodiesel ceases to flow under prescribed conditions. The determination was based on ASTM D2500. The cloud point and pour point were determined visually as the appearance of a 50 mL sample in a 150 mL test jar, where the test jar was put in a bath containing an ice and sodium chloride solution for achieving the low temperature. It can be seen that the pour point and cloud point of the biodiesel was higher than that of petroleum diesel, which may be because of a high level of saturated fatty methyl esters (Table 5). This is why the biodiesel is suitable for warm weather conditions. Research shows that the higher saturated composition will increase the oxidation stability but lower the cloud and pour points⁵³. In contrast, the higher unsaturated composition will enhance the cloud and pour points of biodiesel but lower the oxidation stability⁵³. Compared with the commercial biodiesel, the saturated methyl ester (C16:0 and C18:0) of biodiesel samples was higher, which increased the cloud and pour points.

Table 5 Cloud point and pour point for biodiesels

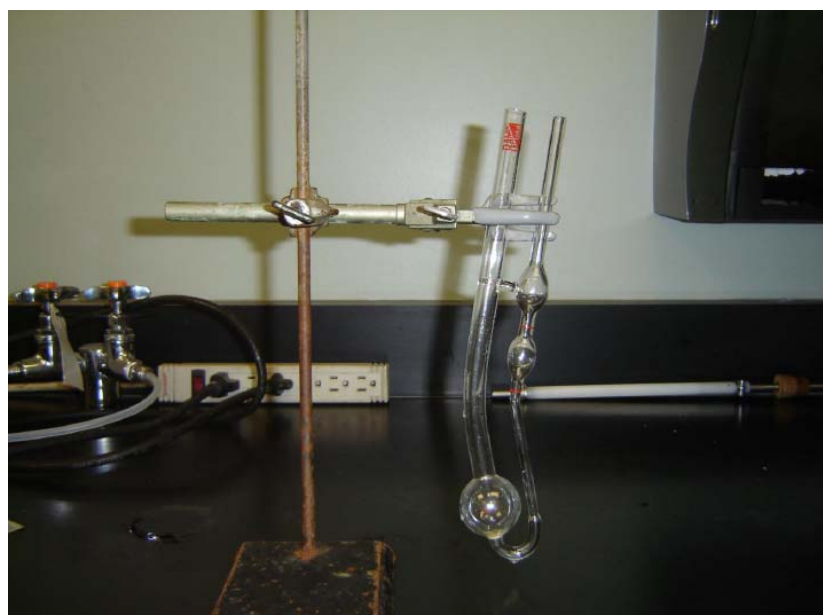
Sample ID	Petroleum diesel	Commercial biodiesel	Sample 1	Sample 2	Sample 3
Cloud point (°C)	-16	4	10	8	9
Pour point(°C)	-33	-5	-1	-3	-2

Kinematic Viscosity. The kinematic viscosity of biodiesel refers to the resistance of a fluid to flow, which is the most important property of biodiesel because good fuels must have suitable flow characteristics to ensure that an adequate supply reaches injectors at different temperatures ⁵⁴. High viscosity can cause problems, such as poor fuel atomization, incomplete combustion and carbon deposits on injectors⁵³. The kinematic viscosity was measured by a viscometer (Ramin, USA) (Fig 8). The viscometer was submerged in a 40 °C water bath and the dynamic viscosity coefficient was 0.0078 cSt at 40 °C. The results showed that that the viscosity of the biodiesel was higher than that of petroleum diesel (Table 6), but they were all within the limits (1.9-6 mm².s⁻¹). The kinematic viscosity of the sample was less than that of commercial biodiesel, which may be due to high content of long chain compounds.

Table 6: Summarized viscosity results of samples

Sample ID	Petroleum diesel	commercial biodiesel	Sample 1	Sample 2	Sample 3
Kinematic viscosity (mm ² s ⁻¹)	2.5-3.5	4.27	4.43	4.4	4.39

Figure 8. Picture of viscometer



Novel Oxygen Carriers for Coal-fueled Chemical Looping

Cetane number. Cetane number is a measurement of the combustion quality of biodiesel during compression ignition. The higher the cetane number, the more ignitable the fuel is. In the present work, ASTM D976 was applied using the fuel density and volatility for the calculation of the cetane number, which gives a reasonably close approximation to cetane number. Testing has shown that this approximates to the regular testing of small volumes or when rapid indications are required for the quality of a diesel fuel, and results are similar to those obtained using more complicated methods⁵⁵. The cetane number is calculated as follows:

$$\text{Calculated cetane number index} = 454.74 - 1641.416D + 774.74D^2 - 0.554B + 97.803(\log B)^2$$

Where D = density at 15°C, g/mL, determined by test method D1298,

B = mid-boiling temperature, °C, determined by test method D86 and corrected to standard barometric pressure.

According to ASTM D6751, the minimum cetane number for biodiesel is 47. Table 7 shows that the cetane number of samples was ranged from 49 to 50. The variation may be due to the distribution of carbon chain lengths in each tested fuel.

Table 7. Summarized cetane number of samples

Sample ID	Conventional diesel	Commercial biodiesel	Sample 1	Sample 2	Sample 3
Cetane number	49-55	49	47	51	54

Acid number. The acid number is the mass of potassium hydroxide (KOH) in milligrams that is required to neutralize 1 g of sample, which is measured using a titration method following ASTM D974. It is good indicator of the level of free fatty acids present in the biodiesel, where a high acid value indicates poorly refined products. It is also an indicator of the quality and the stability of the fuel because the acid number may increase with time as the fuel degrades due to contact with air or water. Table 8 shows that the acid number of the samples was within the limits.

Table 8. Summarized results of acid number for samples.

Sample ID	Petroleum diesel	Commercial biodiesel	Sample 1	Sample 2	Sample 3
Acid number	--	0.23	0.12	0.14	0.17

Novel Oxygen Carriers for Coal-fueled Chemical Looping

Iodine value. The iodine value is the mass of iodine in grams that is consumed by 100 g of biodiesel. It is expressed as grams per 100 g of fat. It is used to determine the amount of unsaturation contained in fatty acids, where the unsaturation is in the form of double bonds that react with iodine compounds. The higher the iodine number, the more unsaturated fatty acid bonds are present in a sample⁵². The iodine value of the samples was within the limits (Table 9).

Table 9. Summarized iodine value of samples.

Sample ID	Commercial biodiesel	Sample 1	Sample 2	Sample 3
Iodine value	118	118	120	119

Gross heating value. Gross heating value is an important property of the biodiesel that determines its suitability as an alternative to diesel fuels. The experiment was performed on Leco AC 600 bomb calorimeter (Fig 9). As can be observed from Table 10, the values ranged from 9370 to 9420 cal g-1 and the gross heating value of the samples was similar to that of commercial biodiesel, but less than that of the petroleum diesel fuel at 10200 cal g-1. With regards to the influence of variables, higher gross heating values were obtained for experiments in which the yields of ester were higher.

Figure 9. Picture of bomb calorimeter.

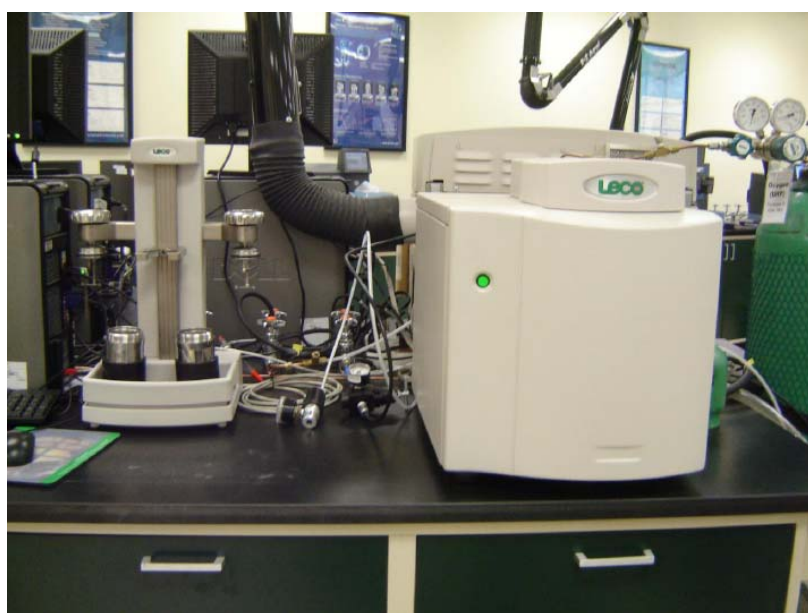


Table 10. Summarized heating value of the samples

Sample ID	Petroleum diesel	Commercial biodiesel	Sample 1	Sample 2	Sample 3
Gross heating value (cal g ⁻¹)	10200	9418	9417	9372	9400

Sulfur, phosphorus, calcium and magnesium content. The measurement of sulfur, phosphorus, calcium and magnesium was measured using ASTM D129. The samples were first oxidized in a bomb calorimeter(Leco AC 600) and then 0.02 g.L⁻¹ Na₂CO₃ was used as an adsorbent. Then the liquid solution was analyzed by a Teledyne Leeman Labs Prodigy ICP-AES (Fig 10). Table 11 shows the summarized ICP results for the samples. Based on the ASTM method, the sulfur content of the samples was within the limits. The P content is about 10 ppm. The Mg²⁺ content was within the limits while the K⁺ and Ca²⁺ content was higher than the limits, but was similar to that of commercial biodiesel, so this needs to be further studied.

Figure 10. The Picture of ICP-AES.



Table 11. Summarized ICP results for samples

Sample ID	S (ppm)	P (ppm)	K (ppm)	Ca (ppm)	Mg (ppm)
Commercial biodiesel	42	10	67	81	5
Sample 1	17	10	69	72	3
Sample 2	44	10	76	98	6
Sample 3	41	11	68	65	1

3.2 Thermal Characteristics Methods

3.2.1 Reagents and Materials

The biodiesel from the soybean oil was obtained using conventional methods. Soybean oil (50 g, 0.056 mol), methanol (10.78 g/ 0.33 mol) corresponding to a 6: 1 ratio of alcohol to oil and KOH (1%, w/w) were refluxed together in a 250 mL glass reactor equipped with a mechanical stirrer. Heating was achieved by means of a water bath. After the mixture reached a temperature of 65 °C, stirring was initiated (600 rpm). After being allowed to react for 1 hour, the mixture was transferred to a separatory funnel and allowed to settle overnight. The upper layer was the coarse biodiesel with catalysts and methanol, while the lower layer was a mixture of glycerol and methanol. The upper layer was vacuum distilled at 80 °C to recover the methanol, washed with hot water (50 °C) until the pH was 7, and then dried with anhydrous sodium sulfate.

For comparison, the biodiesel was also analyzed on a Varian 3800 gas chromatograph fitted with a polar capillary column (Wax 30 m×0.25 mm×0.25 μm, Restek, USA) and a flame ionization detector (GC-FID). The temperature program was as follows: The initial oven temperature was 190 °C, ramping to 200 °C at the rate of 0.5 °C min-1, and then ramping to 240 °C at a rate of 20°C min-1, isothermal for 2 min. The injector and detector temperatures were 220 °C and 230 °C respectively. The split ratio was 50.

3.2.2 Characterization of Bio-Diesel Using Thermal Characteristics Methods

Thermal Stability and Oxidative Stability⁵⁶. The thermal stability measurement was performed in a TA Q5000 TGA. A 10 mg biodiesel was placed in a platinum pan and heated to 600 °C at a heating rate of 10 °C min-1. The experiment took place in an ultra high pure (UHP) nitrogen atmosphere with flow rate of 35 mL min-1. The OOT and OIT were measured using a TA Q20 PDSC. In the OOT experiment, 3 mg of biodiesel was placed in a pinhole aluminum pan and heated to 300 °C at a heating rate of 10 °C min-1. In the OIT experiment, the biodiesel was heated to 110 °C at rate of 10 °C min-1 and then isothermal for 100 mins. Both experiments took place in an oxygen atmosphere under a pressure of 100 psi.

Crystallization Onset Temperature. The crystallization onset temperature was measured on a TA Q2000 DSC. A 10 mg biodiesel was firstly isothermal at -70°C for 5 mins, and then heated to 20 °C at the heating rate of 5 °C min-1. The experiment took place in the UHP nitrogen with flow rate of 50 mL min-1.

Moisture Adsorption. The moisture adsorption experiment took place on a TA Q5000 SA. A 5

Novel Oxygen Carriers for Coal-fueled Chemical Looping

mg biodiesel sample was put in a quartz pan and equilibrated at 25 °C with 0% humidity for 60 mins and then stepwise to 80% with 10% increase in each step, and then desorption from 80% to 10% at a step rate of 10%. The experiment took place in UHP nitrogen atmosphere with flow of 200 mL min-1.

Properties of the Biodiesel. In this study ester content was calculated by using EN 14103 (equation 1). Table 12. shows that the biodiesel was mainly composed of methyl palmitate, methyl stearate, methyl oleate, methyl linoleate and methyl linolenate, in which the unsaturated fatty acid esters accounted for 85%. The purity of the biodiesel was similar to that of the commercial biodiesel.

Table 12. Summarized GC result for the biodiesel

Sample ID	Methyl Palmitate (16:0)	Methyl Stearate (18:0)	Methyl oleate (18:1)	Methyl Linoleate (18:2)	Methyl linolenate (18:3)	Methyl esters content (%)
Biodiesel	10.6	3.6	21.6	55.3	7.8	98.9
Commercial biodiesel	10.1	4.7	20.9	54.5	8.8	99

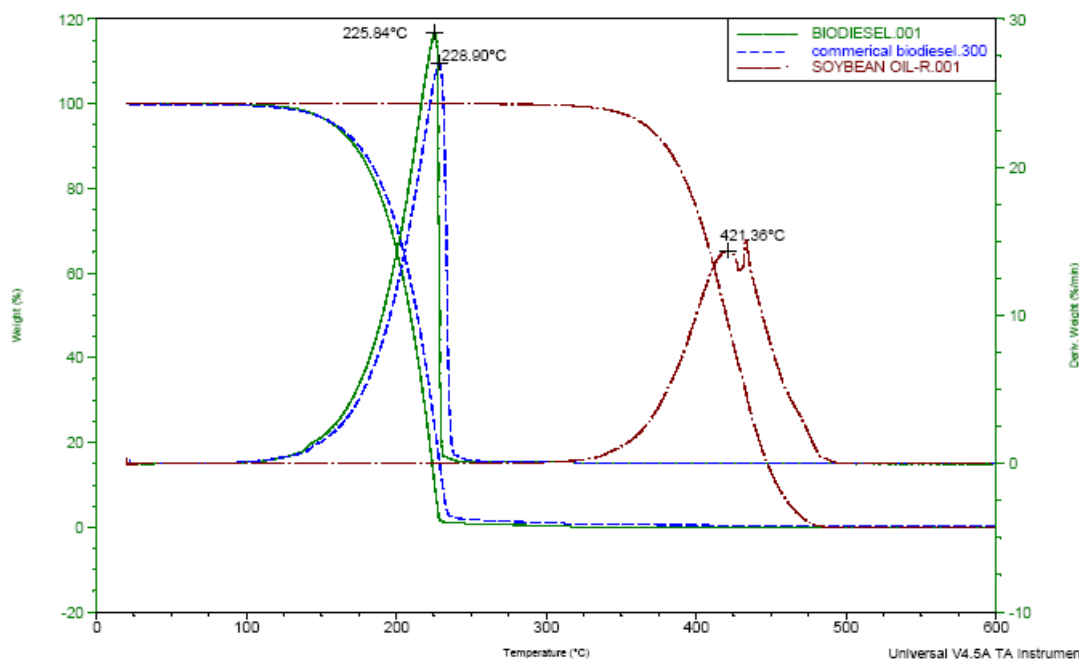
Thermal Stability⁵⁶. Figure 12 shows that there was one weight loss step during the heating of biodiesel in nitrogen flow. Most of the biodiesel was completely decomposed. The onset decomposition temperature of the biodiesel was 193 °C and the onset temperature of the soybean oil was 385 °C (Table 13). After 385 °C, the weight loss of the biodiesel was 0, indicating that there was no soybean oil in the biodiesel, confirming that the biodiesel was pure. The onset decomposition temperature of the biodiesel was similar to that of the commercial biodiesel. The weight loss from 30 °C to 100 °C was 0.1%, indicating that the moisture or water content in the biodiesel was 0.1%.

Table 13 Summarized TGA result for biodiesel and commercial biodiesel

Sample ID	Water content (%) (30-100 °C)	Weight loss(%)	Onset temperature (°C)	Peak temperature (°C)
Biodiesel	0.1	99.9	193	225
Commercial biodiesel	0.3	99.7	196	228
Soybean oil	0.0	100	385	421

Novel Oxygen Carriers for Coal-fueled Chemical Looping

Figure 11. Overlay of TGA curves for biodiesel, commercial biodiesel and soybean oil under N2 flow.



Oxidative Stability⁵⁶. Oxidative stability is very important in the quality control of the biodiesel because biodiesel is mainly composed of unsaturated fatty methyl esters, especially linoleic and linolenic methyl esters, which are more susceptible to oxidation. In this study, the OOT and OIT measurements were based on ASTM E2009 and modified ASTM D 6186. In ASTM D6186, the pressure of 500 psi and oxidative test temperature of 200 °C was specified for measuring the OIT, but if the OIT was under 5 minutes, the temperature and pressures will be altered. In this study, the pressure of 100 psi and the oxidative temperature of 110°C were used to measure the OIT of the biodiesel. PDSC results show that the OOT and OIT of the biodiesel was 152 °C and 24 minutes, respectively, higher than that of the commercial biodiesel, which may be due in part because the biodiesel was fresh while the commercial has oxidative degradation. This observation is similar to other research. Therefore the addition of the antioxidants was very important to the biodiesel.

Novel Oxygen Carriers for Coal-fueled Chemical Looping

Figure 12. OOT curves for biodiesel and commercial biodiesel.

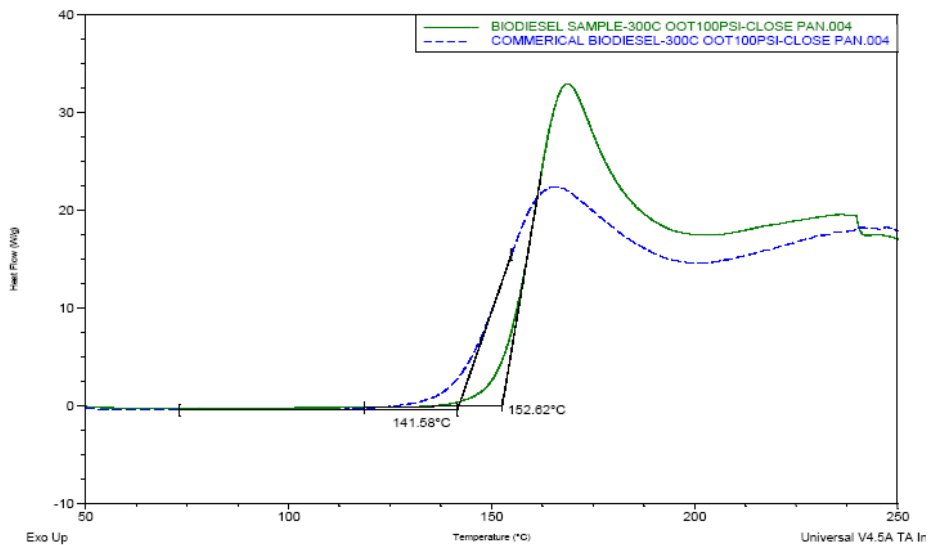
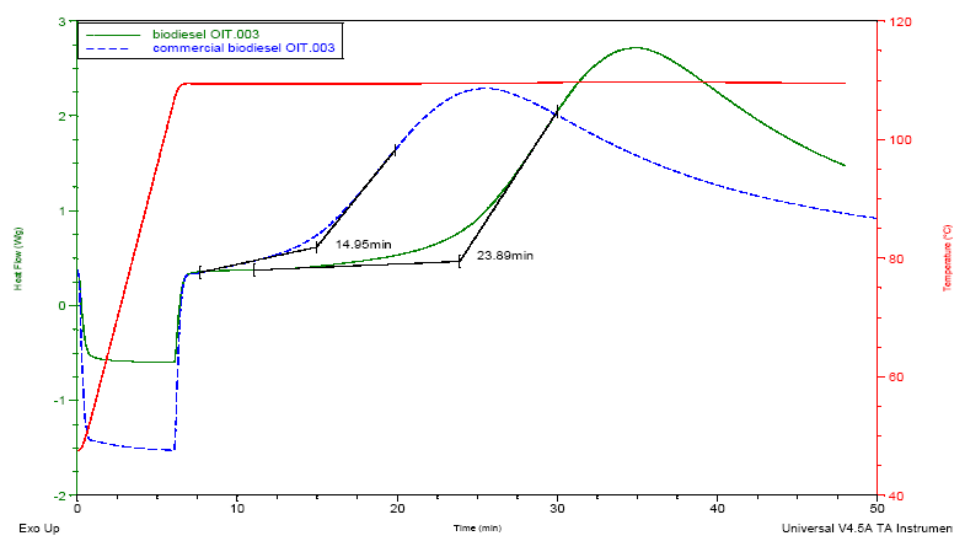


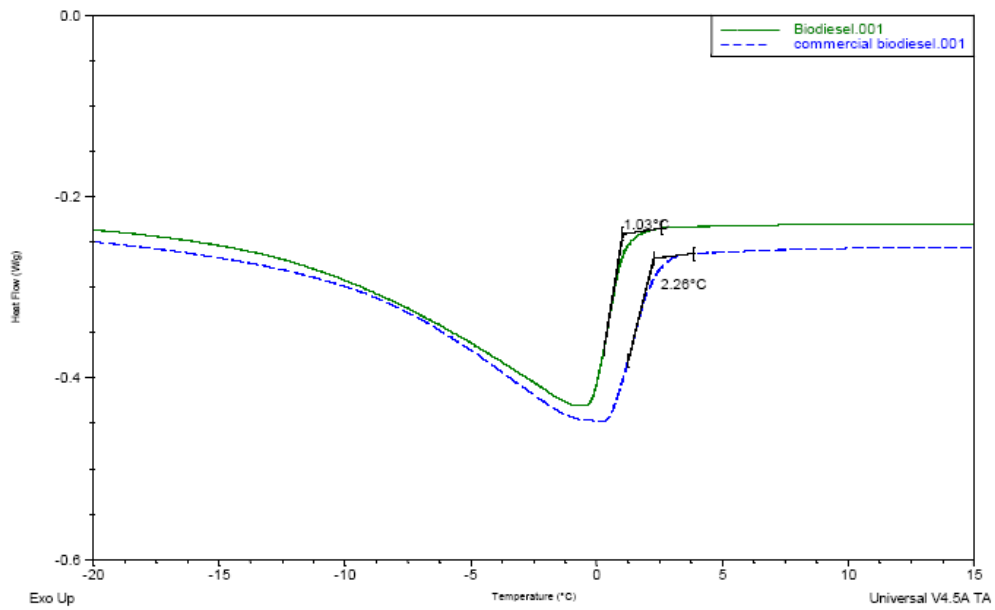
Figure 13. OIT curves for biodiesel and commercial biodiesel.



Crystallization Onset Temperature. High temperature crystallization is another major problem associated with biodiesel. The higher content of unsaturated fatty acid methyl ester force the higher crystallization onset temperature. It can be seen that the onset crystallization temperature of the biodiesel was 1.03 °C, a little lower than that of the commercial biodiesel. As a result, the biodiesel is suitable for cool weather.

Novel Oxygen Carriers for Coal-fueled Chemical Looping

Figure 14. Overlay of DSC curves for biodiesel and commercial biodiesel.



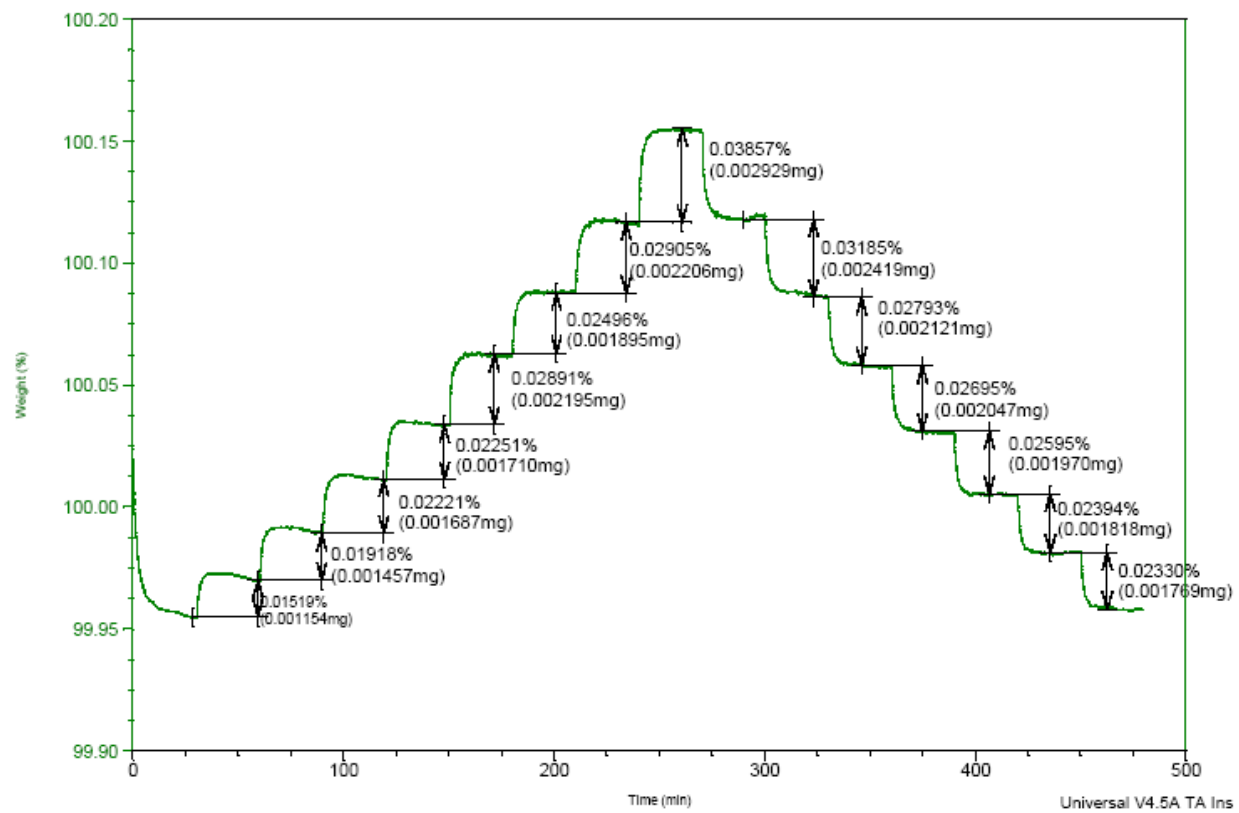
Moisture Absorbing. The functional groups present on the biodiesel have affinity for moisture and therefore it absorbs more moisture than the petroleum oil. The higher moisture content in biodiesel augments microbial growth, causing storage and transportation problems. It can be seen that with increasing humidity, the biodiesel absorbed more water (Table 14). Based on ASTM D6751, the maximum water content was 0.05%, indicating that the better store condition of the biodiesel was in less than 30% humidity. It also can be seen that the water adsorption-desorption was reversible (Figure 15).

Table 14 SA result for biodiesel adsorbing the water

Humidity (%)	Weight gain (%)	Humidity	Weight loss (%)
0 ~ 10	0.015	80 ~ 70	0.038
10 ~ 20	0.019	70 ~ 60	0.031
20 ~ 30	0.022	60 ~ 50	0.027
30 ~ 40	0.022	50 ~ 40	0.026
40 ~ 50	0.028	40 ~ 30	0.025
50 ~ 60	0.024	30 ~ 20	0.023
60 ~ 70	0.029	20 ~ 10	0.023
70 ~ 80	0.038	--	-

Novel Oxygen Carriers for Coal-fueled Chemical Looping

Figure 15. TGA curve for biodiesel under different humidity



4. Effects of Energy Input and Catalysts on Biodiesel Production

The most commonly used method for producing biodiesel is transesterification. This method requires continuous mixing at 55–65 °C for 30-60 min, which requires significant energy consumption. During this process, heat energy is transferred to the reaction through convection, conduction and radiation from the surfaces of the reactor, which has inefficient heat transfer. Large amounts of energy are used to heat the media. Thus, a long reaction time is required to achieve a satisfactory conversion of oil to biodiesel.

An alternative heating system, ultrasonication, has been used in transesterification reactions in recent years, where the transesterification reaction time can be significantly reduced by irradiating the reactants with ultrasonic sound waves at room temperature⁵⁷⁻⁵⁸. Ultrasonic frequencies range from 20 kHz to 10 MHz with acoustic wavelengths in liquids of roughly 100-0.15 mm. When ultrasonic waves are passed through a mixture of immiscible liquids, extremely fine emulsions can be generated. These emulsions have large interfacial areas, which provide more reaction sites for catalytic action, and thus, increase the rate of the transesterification reaction. Low-frequency ultrasonication is a useful tool for emulsification of immiscible liquids, which not only induces an effective emulsification but also mass transfer, so that the rate of ester formation under an ultrasonic mixing condition is higher than that under a stirring condition⁵⁶. During transesterification, methanol is only partially miscible with triglycerides at ambient temperature. The ultrasonic irradiation causes cavitation bubbles near the phase boundary of methanol and oil. The collapse of these cavitation bubbles and micro jets enhance intensive mixing of the system near the phase boundary. Research shows that the collapse of cavitation bubbles produces intense local heating (~5000 K), high pressures (~1000 atm) and enormous heating and cooling rates (>10⁹ K s⁻¹) and liquid jet streams (~400 km/h)⁵⁷. As a result, it provides more energy in a short time and accelerates the reactions. So ultrasonic mixing is an efficient, time-saving and economically method that offers several advantages over the classic procedure⁵⁸.

Heterogeneous catalysts have been paid more and more attention for biodiesel production because these catalysts are not consumed or dissolved in the reaction and therefore can be easily separate from the products. Moreover, they also can be regenerated and reused and it is more environmentally benign because there is no need for acid or water treatment in the separation step⁵⁹. A number of solid bases catalysts have been studied such as metal oxides⁶⁰, metal

Novel Oxygen Carriers for Coal-fueled Chemical Looping

complexes⁶¹, zeolites, Mg-Al hydrotalcites⁶² and support catalysts⁶³⁻⁶⁴. It is worth noting that some of the catalysts were quite expensive or complicated to prepare, which limits their industrial applications. A cheap and easy preparation is necessary for biodiesel synthesis. During the biodiesel synthesis, another major problem associated with heterogeneous catalysts is the formation of three phases with alcohol and oil, which leads to diffusion limitations thus lowering the rate of the reaction. The way of overcoming mass transfer problem in heterogeneous catalysts is using certain amount of co-solvent to promote miscibility of oil and methanol or using intensification methods such as ultrasonic, microwave irradiations and supercritical conditions to improve the biodiesel synthesis processes⁵⁹⁻⁶².

4.1 Effects of Ultrasonic Energy Input

4.1.1 Materials and Methods.

Conventional transesterification was conducted in a 250 mL glass reactor with a condenser. 50 g soybean oil (0.05 mol) was preheated to 65 °C by means of a water bath. Then the prepared mixture of KOH (0.5 g, 1% w/w) and methanol (10.78 g, 0.3 mol) was then added to the reactor. The mechanical stirrer speed was 100, 200, 400 and 600 revolutions per minute (rpm), respectively. In order to study the factors of input energy, the reaction time varies from 5 min to 60 min. After completion of the reaction, the mixture was transferred to a separating funnel and settled overnight. The upper layer was the mixture of coarse biodiesel with catalysts and methanol, while the lower layer was a mixture of glycerol and methanol. After separation of the two layers by sedimentation, the upper methyl esters were washed with hot distilled DI water. Finally, the residual water was eliminated by treatment with Na₂SO₄ followed by filtration, and then the methyl esters were ready for GC analysis.

The ultrasonic experiments were performed with an ultrasonic processor UP400S (Hielscher, U.S.A) of 24 kHz with a maximum power of 400 W (Figure 16.). The acoustic intensity was 105 W/cm². The same amounts of the reagents were transferred into a conical flask, and then subjected to ultrasonic synthesis. The experiments were started in the ultrasonic reactor initially at room temperature. Since the temperature of the reactor was not controlled, the temperature rose up to 95 °C during the 5 min duration of the experiment depending on the amplitude setting. The amplitude and the pulse for the reaction were adjustable from 20 to 100% and from 0 to 1, respectively. The titanium sonotrode (H14) with a diameter of 14 mm and a length of 90 mm was

Novel Oxygen Carriers for Coal-fueled Chemical Looping

used to transmit the ultrasound into the liquid. The sonotrode was submerged up to 15 mm into the solution. After completion of the reaction, methyl esters were purified and dried according to the previous procedure. The energy input during the experiment was calculated by equation 1.

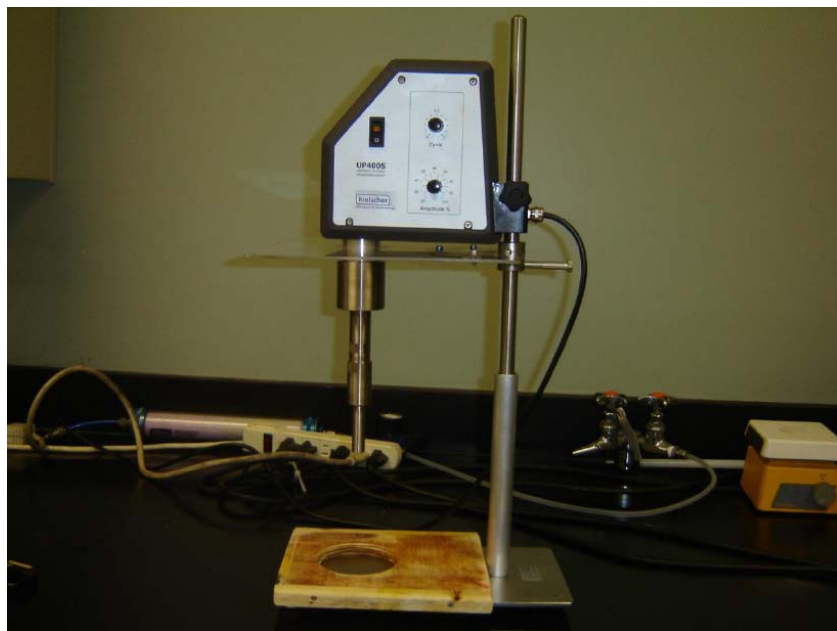
$$E = I \times (\Pi \times d^2/4 + \Pi \times d \times H) \times A \times t \quad (1)$$

Where E is the total input energy (J), I is the acoustic power density (Wcm-2), d is diameter of the sonotrode (cm), H is the immersgence depth in the solution (cm), A is percent of amplitude (%) and t is the total reaction time (s).

The methyl esters were analyzed by a Varian 3800 GC. The ester content was calculated based on EN 14103. Methyl undecanoate was added as an internal standard into the biodiesel samples. The analysis of biodiesel by GC was carried out by dissolving 125 mg of methyl mixture sample in to 2.5 mL of methyl undecanoate (5 mg ml-1), and injecting 1 uL of this solution into the GC. The concentration of the methyl undecanoate was controlled by calibration curve of methyl undecanoate (Figure 17.). The GC conditions were the same as in previous report. The ester content of the biodiesel was calculated according to equation 2.

$$C = \frac{A}{A_{EI}} \times \frac{C_{EI} \times V_{EI}}{m} \times 100\% \quad (2)$$

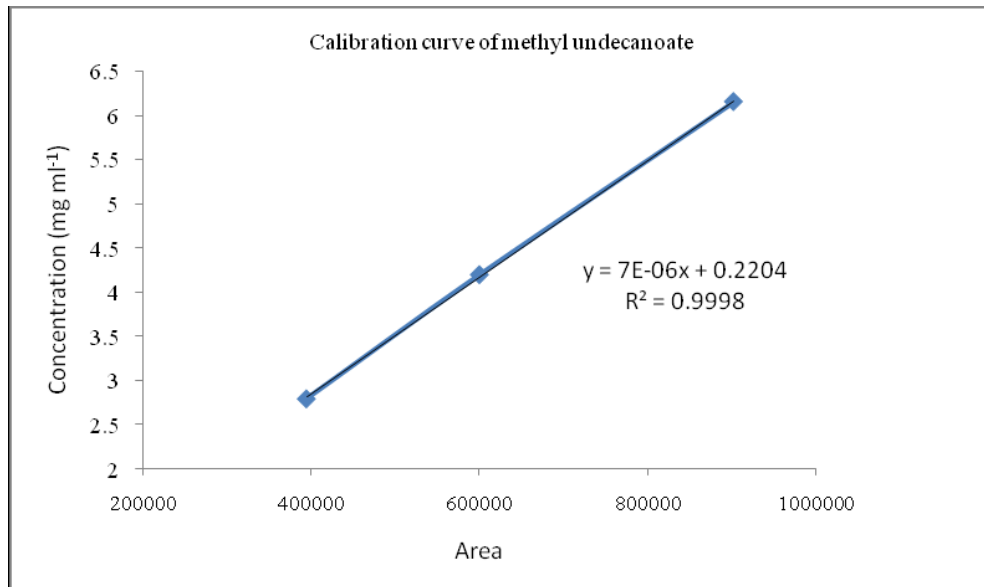
Figure 16. Picture of Sonicator UPS 400.



Novel Oxygen Carriers for Coal-fueled Chemical Looping

Where A is the total peak area from the methyl ester in C14 to that in C24:1; AEI is the peak area corresponding to methyl undecanoate; CEI is the concentration of methyl undecanoate (mg ml⁻¹); m is the mass of the biodiesel sample.

Figure 17. Calibration curve for internal standard-methyl undecanoate



The conversion of oil in each experiment was calculated from the content in methyl esters of biodiesel as analyzed by GC, and the material balance of the reaction:

$$\text{Yield}(\%) = \frac{\text{mass of ester layer after separation}}{\text{total mass of reactant at reaction start}} \times \text{biodiesel concentration} (\%) \quad (3)$$

4.1.2 Comparison of Conventional and Ultrasonication Methods.

A set of experiments was carried out to determine the effect of ultrasonication versus mechanical stirring on the transesterification reaction. In the conventional method, stirring can play an important role in the yield of biodiesel production. Yields of methyl esters isolated by conventional transesterification using mechanical stirring are given in Table 15.. It can be seen that when the reaction time was 60 min, the biodiesel concentration was more than 96.5 % regardless of the stirring speed, indicating that the biodiesel quality meets the standard EN14103. However, the biodiesel yield was only 83-86 %, similar to that found by other researchers. When the stirring speed was 100 rpm, the biodiesel yield was 83.2 %, and only increased by 0.6%

Novel Oxygen Carriers for Coal-fueled Chemical Looping

when the speed was 200 rpm (Figure 18.). After the stirring speed increased to 400 rpm, the biodiesel yield quickly increased to 85.6%. The biodiesel yield at 400 rpm and 600 rpm was similar. Totally the biodiesel yield was 83 % ~ 85 %. It can be seen with increasing stirring speed, the biodiesel yield gradually increased.

Table 15. Biodiesel yield at different stirring speed

Temperature (°C)	Stirring speed (rpm)	Biodiesel yield (%)	Biodiesel purity (%)
65°C, reaction time 60 mins	100	83.2	98.6
	200	83.8	98.3
	400	85.6	99.1
	600	85.8	99.0

Reaction time is very important parameter for biodiesel synthesis. To investigate the effect of the reaction time on the biodiesel yield, the reaction time of 5 min, 15 min, 30 min and 60 min was chosen for analysis (Table 2). It can be seen that with increasing reaction time, the biodiesel yields increased whenever the stirring speed was 200 or 400 rpm. However, the reaction time had more effect at 200 rpm. When the stirring speed was 200 rpm and the reaction time was 5 mins, the biodiesel yield was only 72 %. But when the reaction time increased to 15 mins, the biodiesel yield dramatically increased to 80 %. When the stirring speed was 400 rpm and the reaction time was 5 min, the biodiesel yield was 84.1%, indicating that high stirring speed provides more energy. But after 5 min, the biodiesel yield increased slowly (Figure 4). This also confirms that the when the stirring speed was 400 rpm, it provide more input energy and a better mixing, which accelerates the reaction speed.

It can be seen that the amplitude of sound waves had a large effect on the transesterification reaction (Table 17.). Table 3 shows that regardless of the amplitude, the biodiesel concentration was more than 96.5 %, meeting the EN14103 standard. It also can be seen that when the amplitude was 25 %, the biodiesel yield was 88.8% When the amplitude increased to 75 %, the biodiesel yield reached the maximum, 92.2 %. As the amplitude was increased to 100 %, the biodiesel yield had a small decrease (Figure 20.). It also can be seen that with increasing the amplitude, the solution temperature increased, indicating that ultrasonication not only accelerated the reaction but also increased the solution temperature. But when the reaction time was 10 min

Novel Oxygen Carriers for Coal-fueled Chemical Looping

at 50% of amplitude, the biodiesel yield did not increase. However, the solution temperature still increased, suggesting more energy may not promote the reaction or some methyl esters were cracked or oxidized to short-chain compounds at higher temperature.

Figure 18. Effect of stirring speed on biodiesel yield

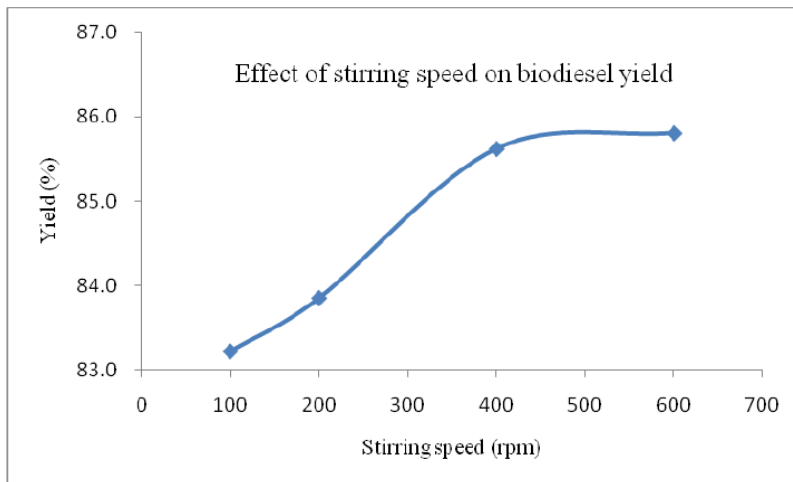
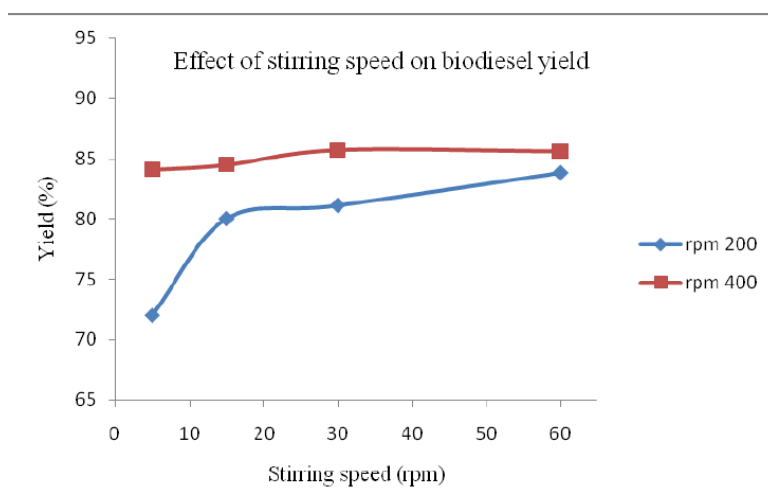


Table 16. Biodiesel yield at different time under same stirring speed

Temperature (°C)	Reaction time (min)	Biodiesel yield (%)	Biodiesel purity (%)
65 °C and rpm at 200	5	72.0	83.9
	15	80.0	97.5
	30	81.1	96.7
	60	83.8	98.3
65°C and rpm at 400	5	84.1	96.6
	15	84.5	97.4
	30	85.7	98.2
	60	85.6	99.0

Figure 19. Effect of reaction time on biodiesel yield.



Novel Oxygen Carriers for Coal-fueled Chemical Looping

Table 17. Biodiesel production under different amplitudes

Amplitude (%)	Reaction time (min)	Input energy (J)	Biodiesel yield (%)	Biodiesel purity (%)	Temperature (°C)
25	5	64044	88.8	98.8	68
50	5	128088	90.9	97.1	76
75	5	192133	92.2	98.2	90
100	5	256177	91.4	98.6	95
50	10	256177	89.3	97.8	118

The input energy of each experiment was different because of different amplitudes and reaction times. The effect of input energy on biodiesel yield is shown in Figure 6. It can be seen that when the reaction time was 5 min, with increasing amplitude and reaction time, the input energy increased, while the biodiesel yield did not have the same trend. When the amplitude was 25 %, the input energy was 64044 J and the biodiesel yield was 88.8 %. When the amplitude was 75 %, the input energy was three times that at 25 % amplitude, and the biodiesel yield also increased to 92.2 %. When the amplitude was 100 %, the input energy was four times that at 25 % amplitude, but the biodiesel yield decreased to 91.4%. When the amplitude was 50 % and the reaction time was 10 min, the input energy was the same as that at 75 % amplitude and the biodiesel yield was 89.3%. It is known that more energy will accelerate the reaction, but this data contradicts that. This may be because during experiment the temperature of the ultrasonic reactor was not controlled. As a result, the solution temperature increased quickly, which prevented the reaction between the methanol and oil because at high temperature the methanol became a gas. Another reason may be that the formed methyl esters cracked or oxidized to low-weight organic fractions at high temperature. This further suggests that the suitable temperature for synthesizing biodiesel is 50~80 °C.

Figure 20. Effect of amplitude on biodiesel yield

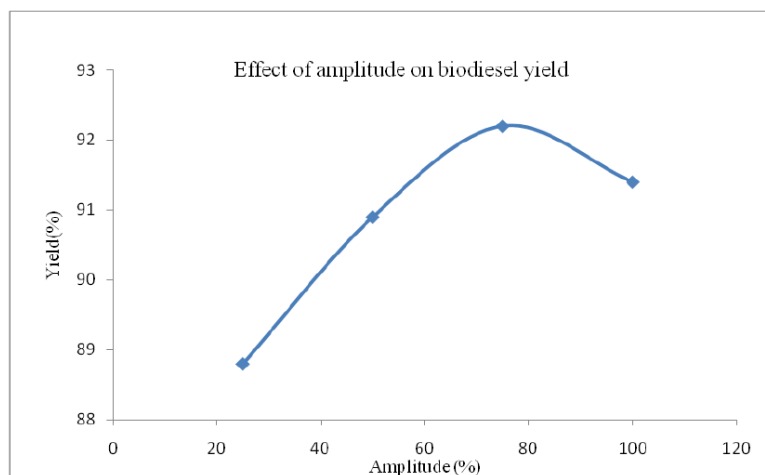


Figure 21. Effect of input energy on biodiesel yield

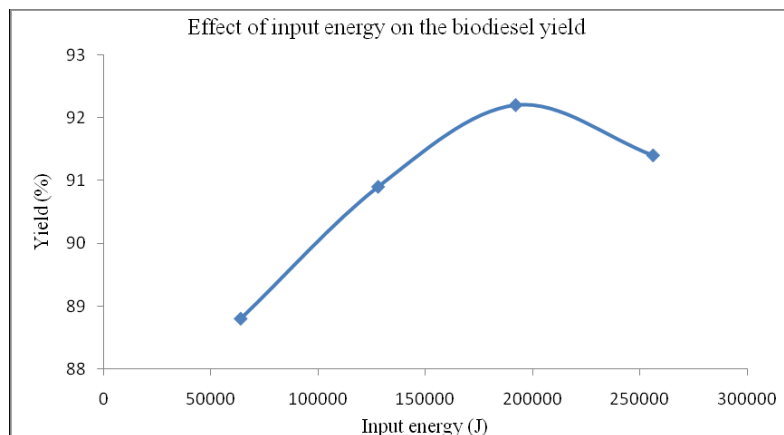


Table 18. Summarized ester content of the biodiesel under different catalysts

Sample ID	Reaction time (min)	Purity (%)
SrO as catalyst	10	74
CaO as catalyst	10	9
γ -Al ₂ O ₃ as catalyst	10	0

4.2 Effects of Heterogeneous Catalysts

4.2.1 Materials and Methods

Methanol of purity >99.9%, K₂CO₃, SrO, BaO and CaO were purchased from Fisher, USA. γ -Al₂O₃ was purchased from SASOL Germany GmbH.

The impregnation method and dry method was used to prepare the catalysts. In dry method, γ -Al₂O₃ was used as substrates and CaO, K₂CO₃ was used as carrier. The substrate and carrier was mixed with the ratio of 1:1 in a mortar. After mixing, the mixture was calcinated for 2 hrs at designed temperature. In the impregnation method, the γ -Al₂O₃ was put in the aqueous solution of K₂CO₃ and KOH for 12 h. Then the solution was put in the hot plate until the solution was drying with stirring. After that the mixture was calcinated in a muffle oven at desired temperatures (usually 800°C) for 2 hrs.

All the catalytic tests were carried out using the same experimental conditions so that maximum conversion in terms of methyl esters is obtained. The reaction was carried out in a 250 mL three-necked round-bottomed flask equipped with a immersed thermometer, a reflux

Novel Oxygen Carriers for Coal-fueled Chemical Looping

condenser and a an ultrasonic processor UP400S (Hielscher, U.S.A) (Figure 22.). The flask was immersed in a water bath. The temperature was controlled by intermittently adding ice. The amplitude and the pulse of the ultrasonic processor for the reaction were set to 100% and 1, respectively. The titanium sonotrode (H22) with a diameter of 14 mm and a length of 150 mm was used to transmit the ultrasound into the liquid. The sonotrode was submerged up to 20 mm into the solution. Typically, 50 g soybean oil (0.05 mol), methanol (the ratio of methanol to oil was 12:1 or 18:1) and 4 % catalyst (w/w, oil basis) was transferred to the reactor for reaction. In After reacting for 60 min, the mixture was cooled and centrifuged for 30 mins, where it formed three phases. The top layer was biodiesel, the middle was the glycerol and the bottom was catalyst. Then the methanol was recovery by vacuum distillation. After recovery, the biodiesel was analyzed by GC 6890 with the internal standard (methyl undecanoate) method. In the experiment, in order to quickly compare the effect of the catalysts, only the methyl esters content of the solution was compared. The conversion rate of the biodiesel will be analyzed later.

Figure 22. Schematic for experiment setup



4.2.2. Comparison of Conventional homogeneous and Heterogeneous Methods

Table 19 shows the biodiesel yields by using different solid catalyst. From Table 19. it can be seen that the dry method was better than the impregnation method, where the biodiesel yield increased by 40%. So in the later study, the dry method was used for preparing the catalysts.

It can be seen that BaO and SrO have the high reactivity and high yield, especially SrO, the

Novel Oxygen Carriers for Coal-fueled Chemical Looping

purity reached 97% in 30mins. However, these metal oxide have high corrosiveness and expensive. The reactivity of CaO was lower, even when the molar ratio of oil to methanol increased to 1:18, the biodiesel purity was only 38%. However, CaO was the cheapest biodiesel, so the next step was to provide more energy to promote the reaction.

K_2CO_3 shows a good performance for catalyzing the reaction, where the biodiesel yield was 94% in 60 minutes. When the γ - Al_2O_3 was used as supporter, the biodiesel yield increased to 97%. This is because γ - Al_2O_3 has the larger surface area ($155\text{ m}^2/g$), which accelerated the biodiesel synthesis. It also can be seen that when the ratio of Al_2O_3 to K_2CO_3 decreased to 1:0.5, the biodiesel yield was 94%, indicating that the amount of K_2CO_3 can be reduced. It's a potential catalyst.

Another interested catalyst was the mixture of KOH and $Al_2Si_2O_5(OH)_2$, where purity of the biodiesel reached 99% in 60 mins. As we know $Al_2Si_2O_5(OH)_2$ come from the clay, which is the cheap source, so it will be continued to be studied. From above all, it can be seen some catalysts have good effect, but it hasn't been reused. So the next step is to continue to develop more catalysts and consider the economic effect.

Table 19. Summarized biodiesel yield for different catalysts

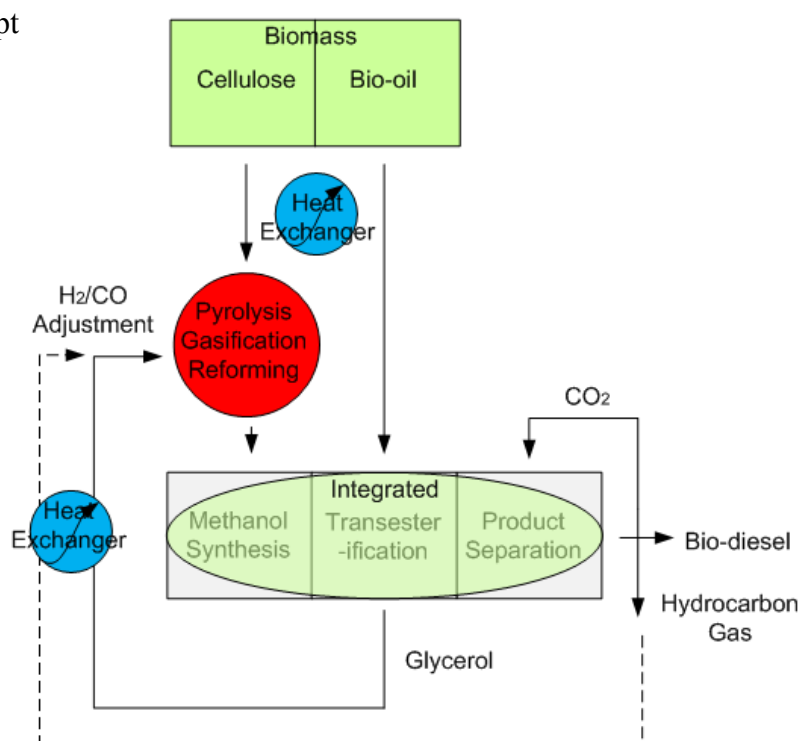
Catalyst	Catalyst amount (%)	Reaction time (min)	Oil:MeOH ratio	Purity (%)
γ - Al_2O_3	4%	60	1: 12	0
γ - Al_2O_3	8%	60	1: 12	0
CaO	4%	60	1: 12	0
CaO	4%	60	1:18	38
BaO	4%	45	1: 12	93
SrO	4%	30	1: 12	97
K_2CO_3	4%	60	1: 12	95
γ - Al_2O_3 loaded KOH (1:1)-impregnation method	4%	60	1: 12	51
γ - Al_2O_3 loaded K_2CO_3 (1:1)-dry method	2%	60	1: 12	90
γ - Al_2O_3 loaded K_2CO_3 (1:1)-dry method	4%	60	1: 12	94
γ - Al_2O_3 loaded K_2CO_3 (1:0.5)	4%	60	1: 12	94
γ - Al_2O_3 loaded K_2CO_3 (1:1)	4%	60	1: 12	97
KOH and $Al_2Si_2O_5(OH)_2$ (1:1) 1000°C	4%	60	1:12	99

5. Feasibility of Process Couplings

5.1 Process Basics

The conceptional development of this advanced bio-diesel production process is shown in Figure 23. In the area marked with red in Figure 23, the cellulose-based biomass will be used as primary feedstock to produce the synthesis gas ($H_2 + CO$ plus CO_2) in the steam gasification process. Synthesis gas is purified and delivered, together with bio-oils, to the coupling and separation reactor to conduct coupling process of methanol synthesis, bio-oil transesterification and bio-diesel separation. This is shown in the light green area of Figure 23. Some of exothermic energy heat in methanol synthesis is taken by the endothermic transesterification of cold-feed bio-oil and endothermic gasification processes. The byproduct from coupling process of bio-oil transesterification and methanol synthesis, such as methane and low hydrocarbon and glycerol, can be supplied to the co-gasification process to provide additional H_2 source through reforming process. Thus, the H_2/CO ratio can be adjusted to produce the stoichiometrically feasible synthesis gas of F-T process. In such coupling design of process, the heat transfers are intensified because of its in-site properties, and oxygen production could be excluded in the process because of couplings of endothermic and exothermic reactions. In such coupling design of process, byproducts from coupling reactions could be potentially utilized at their maximums.

Figure 23. Process concept



Novel Oxygen Carriers for Coal-fueled Chemical Looping

In this coupling process, supercritical methanol conditions and catalyst selection are two major measures to make the proposed process integration potential feasible.

A few studies reported the successful non-catalytic transesterification under supercritical methanol conditions (250–400 K and 15–35 MPa)^{66–72}. Compared with conventional catalytic processes under barometric pressure, the supercritical methanol process is non-catalytic, is much simpler to purify the products, has improved reaction kinetics, is more environmentally friendly and is lower in energy use. There are several other advantages of supercritical methanol transesterification over the conventional transesterification process. 1) Supercritical methanol has a high potential for both transesterification of triglycerides and methyl esterification of free fatty acids to methyl esters; and 2) the presence of water positively affected the formation of methyl esters in the supercritical methanol method⁶⁹, which is much different from water's function in the traditional transesterification process. Methanol synthesis was initially conducted using ZnO–Cr₂O₃ catalyst under 350–400 °C and 24–30 MPa. The conversion reactions are, therefore, thermodynamically favored by low temperatures and high pressures. Numerous improvements have been pursued to reduce investment costs via dropping operational pressures⁷³. Low pressure operation is presently favored in methanol synthesis due to its low cost. But, it tends to result in a low fraction of the synthesis gas being converted in each pass (typically about 10 % conversion efficiency). Compatiability of operational conditions of two reactions seemed critical for coupling process. Several commercially available methanol synthesis catalysts were selected to evaluate their one-pass conversion efficiency, compatibility to synthesis gas with various H₂/CO ratios, and operational temperatures and pressures compatible to the supercritical bio-oil transesterification. The basic reaction enthalpies, chemical equilibrium and chemical reaction kinetics for bio-oil transesterification and methanol synthesis via synthesis gas were studied.

To achieve controlling variable high pressure conditions, two high-pressure test rigs (100–500 ml/min) were designed and setup to carry out the proposed coupling tests. Tests include 1) correlation and compatibility of coupling reactions under variable temperatures and pressures; 2) conversion efficiency of selected bio-oil, conversion efficiency of synthesis gas, consumption rate of methanol by bio-oil transesterification and constitutes of byproducts under various temperatures and pressures; 3) quality of bio-diesel products including their purity and unexpected byproducts in product mixture; 4) starting with commercial available methanol synthesis catalysts, performance evaluation of self-prepared catalysts in integration reactions on

yield of target products.

5.2 Setup of High-pressure Biodiesel Production Facilities

Bench Scale Stirring Catalytic Reactor

A PARR bench scale stirring catalytic reactor system has been setup. This system could be operated flexibly in a bench non-continuous feeding mode or a continuous-feeding-discharging mode, the experimental medium could be either gas-liquid or liquid-liquid. The volume of the reactor is 500 mL. The designed temperature could reach as high as 350°C, and the pressure could reach as high as 350 bar. The catalyst cage inside could hold as much as 1 to 20 grams of catalyst. The high pressure liquid injection pump could achieve the liquid injection rates precisely as 0.01 g per minutes and 20 grams per minutes as maxim. This bench scale high pressure system was shown in Figure 24.

Figure 24. The bench scale stirring catalytic reactor system



Continuous-flow reactor

A continuous-flow high pressure reactor system has also been setup. This system could also be operated flexibly in a continuous-feeding-discharging mode, and the experimental medium could be either gas-liquid or liquid-liquid. The volume of the reactor is 250 mL. The designed temperature could reach as high as 350°C, and the pressure could reach as high as 350 bar. The maximum speed of stirring could reach 3500 rpm. The catalyst cage inside could hold as much as 1 to 20 grams of catalyst. The high pressure liquid injection pump could achieve the liquid injection rates precisely as 0.01 g per minutes and 20 grams per minutes as maxim. This bench scale high pressure system was shown in Figure 25.

Figure 25. The continuous-flow high pressure reactor



Thermal Analysis for Quick Determination of Bio-diesel conversion efficiency

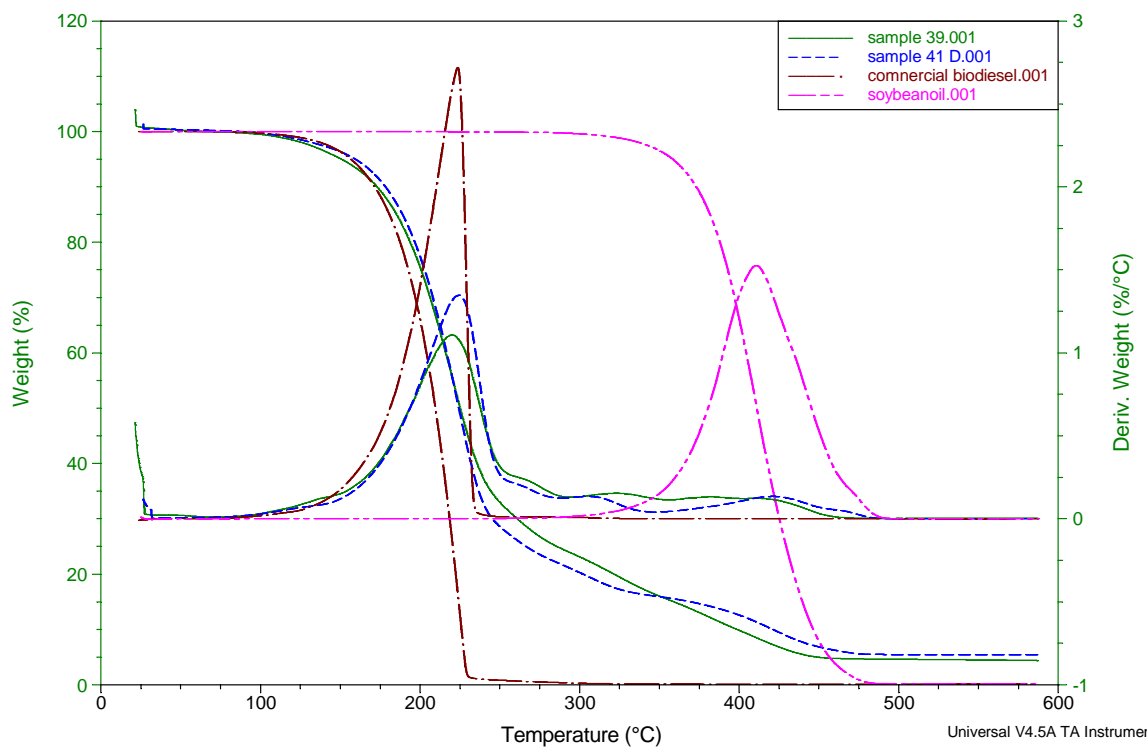
The product samples, after reacting under high pressure and temperature conditions, generally split into two portions with significant differences in their densities, which are easily separated. The portion on the top layer in the split with a lower density generally corresponded to unreacted methanol and bio-oil and produced biodiesel, whereas the portion at the bottom layer in the split with higher density corresponded to the unreacted methanol and byproducts. The reactor contents were completely transferred into a flask and freed of methanol and volatiles at the reduced pressure in a rotary evaporator. The remaining products were centrifuged (5000 rpm) for 15 mins for the separation of bio-diesel product (mixed with bio-oil) and byproduct (mainly glycerol). The regular static separation of bio-oil and the produced biodiesel was not deemed

Novel Oxygen Carriers for Coal-fueled Chemical Looping

effective. The all high pressure transesterification conditions, the lower ratio of methanol and bio-oil were applied at 6.

A novel thermal analysis method has been developed to quickly evaluate the conversion efficiencies for the reaction between methanol and bio-oil (soybean oil in this study). The commercially available biodiesel and soybean oil samples demonstrated significantly different typical weight loss peaks in the 30-600 °C temperature range, as shown in Figure 26. A single weight loss peak at 235 °C corresponds to biodiesel, where as a single weight loss peak at 430 °C corresponds to bio-oil. Any mixture samples, containing biodiesel and bio-oil, will present the aforementioned two typical weight loss peaks. Their weight loss at different temperature ranges represents conversion efficiencies of methanol and bio-oil.

Figure 26. Overlay of TGA curves for samples 39, 41, commercial biodiesel and soybean oil.



For confirmation on the conversion efficiencies using our novel thermal analysis method, an ASTM method based on the GC instrumentation was also conducted. The biodiesel (FAME) was analyzed by a Varian 3800 gas chromatograph fitted with a polar capillary column (Wax 30 m×0.25 mm×0.25 μm, Restek, USA) and a flame ionization detector (GC-FID). The temperature

Novel Oxygen Carriers for Coal-fueled Chemical Looping

program was as follows: The initial oven temperature was 190 °C, ramping to 200 °C at the rate of 0.5 °C min⁻¹, isothermal for 20 min, and then ramping to 240 °C min⁻¹ at the rate of 20 °C min⁻¹, isothermal for 2 min. The injector and detector temperatures were 220 °C and 230 °C respectively. The split ratio was 50. The sample was diluted and injected with a volume of 1.0 µL. The calculation of ester content was based on EN14103.

5.3 Process Couplings

Supercritical methanol transesterification

A total of 52 biodiesel samples have been obtained, covering conditions of different temperatures, pressures, and residence times of reaction between methanol and bio-oil, using any catalysts. For all tests, the ratios of methanol and bio-oil were maintained as low as 6. Results were presented in Table 20. The quality of obtained bio-diesel samples (Samples 39 and 41) were presented in Figure 26.

Table 20. Bio-diesel production under supercritical conditions

Sample Number	1	2	3	4	5	6	7	8	9	10	11
Temperature (C)	250	250	room	100	200	room	350	350	350	350	300
pressure (bar)	100	100	non	non	non	150	non	150	100	200	200
Time (hr)	1	0.5	2	1	1	1	1	1	1	1	1
Catalyst	Cu/Zn/Al										
Gas	N2										
Condition	MeOH										
String Speed	150rpm										
Conversion	93.67	87.6	0.3377	0.3251	41.32	1.659	60.32	67.06	69.82	66.66	89.85

Sample Number	12	13	14	15	16	17	18	19	20	21	22
Temperature (C)	300	300	250	250	350	250	260	250	250	300	250
pressure (bar)	150	100	150	200	200	100	100	200	100	100	200
Time (hr)	1	1	1	1	1	1	1	1	0.5	1	1
Catalyst	Cu/Zn/Al										
Gas	N2	N2	N2	N2	CO2	CO2	N2	CO2	CO2	N2	N2
Condition	MeOH	MeOH	MeOH	MeOH	MeOH	MeOH	MeOH+H2O	EtOH	EtOH	EtOH	EtOH
String Speed	150rpm	150rpm	150rpm	1500rpm	150rpm	150rpm	300rpm	150rpm	150rpm	150rpm	150rpm
Conversion	88.45	89.67	94.47	94.75	74.68	93.89	95.38	91.21	82.87	85.82	91.43

Sample Number	23	24	25	26	27	28	29	30	31	32	33
Temperature (C)	300	300	250	250	250	250	250	250	250	300	250
pressure (bar)	200	200	200	200	200	200	200	non	200	250	200
Time (hr)	1	0.5	0.5	1	1	1	1	1	1	1	1
Catalyst	Cu/Zn/Al	Cu/Zn/Al	Cu/Zn/Al	Cu/Zn/Al 650c-Y	Cu/Zn/Al 400c-r	Cu/Zn/Al 650c-Y	Cu/Zn/Al 400c-r	no	Cu/Zn/Al	Cu/Zn/Al	Cu/Zn/Al 400c-r
Gas	N2	N2	N2	N2	N2	N2	N2	N2	N2	N2	N2
Condition	EtOH	EtOH	EtOH	MeOH	MeOH	EtOH	EtOH	MeOH+H2O	MeOH+H2O	MeOH+H2O	MeOH+H2O
String Speed	150rpm	150rpm	150rpm	150rpm	150rpm	150rpm	150rpm	150rpm	150rpm	150rpm	150rpm
Conversion	89.04	86.28	84.72	94.27	94.69	89.57	89.3	28.24	93.69	93.04	94.99

Novel Oxygen Carriers for Coal-fueled Chemical Looping

Sample Number	34	35	36	37	38	39	40	41	42	43	44
Temperature (C)	250	220	285	285	285	260	375	275	245	250	230
pressure (bar)	200	50	250	300	300	100	230	250	90	250	75
Time (hr)	3	1	1	1	1	1	1	1	1	1	1
Catalyst	Cu/Zn/Al										
Gas	N2	N2	N2	N2	N2	CO2	N2	N2	N2	N2	CO2
Condition	EtOH+H2O	MeOH+H2O	MeOH+H2O	MeOH+H2O	EtOH+H2O	MeOH	MeOH+H2O	MeOH+H2O	MeOH+H2O	MeOH+H2O	MeOH
Stringing Speed	150rpm	500rpm	150rpm								
Conversion	87.74	88.04	93.76	94.77	88.55	95.38	70.47	95.92	89.97	92.15	91.24

Sample Number	45	46	47	48	49	50	51	52
Temperature (C)	250	33	275	300	275	275	275	275
pressure (bar)	80	60	70	90	250	100	100	250
Time (hr)	1	2	1	1	2	2	4	1
Catalyst	Cu/Zn/Al	Cu/Zn/Al	Cu/Zn/Al	Cu/Zn/Al	Cu/Zn/Al	Cu/Zn/Al	Cu/Zn/Al	Cu/Zn/Al
Gas	CO2	CO2	CO2	CO2	N2	N2	N2	N2
Condition	MeOH	MeOH	MeOH+EtOH	MeOH+EtOH	MeOH	MeOH	MeOH	oil:MeOH:H2O=1:24:1
String Speed	150rpm	150rpm	150rpm	150rpm	150rpm	150rpm	150rpm	150rpm
Conversion	93.21	0.68	83.77	86.36	92	91.74	86.67	92.68

The initial search for the optimum pressure conditions for the increased production of biodiesel seemed infeasible, at least for pressures up to 250 bar. Typical temperatures and residence times used while adjusting pressures were in the range of 25 °C to 150 °C and 0.5 hours to 2 hours. The search for the optimal temperature conditions on the promotion of the biodiesel productivity lead to a significant increase in conversion efficiencies when the temperature was increased to about 250 °C. It appears that the effect of the temperature is more significant than that of the pressure. Further increasing of temperature, such as 300 °C, did not significantly increase the bio-oil conversion as expected. While maintaining 250 °C and dropping the pressure to mild conditions (80-100 bar), the conversion efficiencies of biodiesel were even improved. For example, as the temperature was kept constant at 250 °C with a residence time of 1 hour, the increase of pressures from 80 bar to 200 bar did not improve the conversion efficiencies. Currently the best results under conditions of high pressure and temperature, such as sample 39 (T= 260 °C, P= 100 bar, rpm= 150, Time= 1 hrs) and sample 41 (T= 275 °C, P= 250 bar, rpm= 150, Time= 1 hrs), have yielded conversion efficiencies about 95% under the ratio of methanol and bio-oil only at 6. Under supercritical conditions, water did not impact negatively on the bio-diesel conversion efficiencies. This was completely different from the case when occurrence of transesterification under the ambient pressure. Further increase the ratio of

Novel Oxygen Carriers for Coal-fueled Chemical Looping

methanol and bio-oil could significantly increase the kinetics of the bio-oil conversion efficiency to above 99% within 10 mins. The current tests clearly demonstrate the effect of temperature and pressure on the conversion of the bio-oil and the methanol. This is a positive first step in our approach for the coupling reaction of biodiesel production under high pressure and temperature. The Quality of obtained bio-diesel samples were shown in Table 21, which were comparable to the commercial bio-diesel samples.

Table 21. Summary of Qualities of Produced Bio-diesel under supercritical methanol conditions

	Sample 39	Sample 41	Biodiesel	ASTM standard
Density (g/cm3)	0.895	0.89	0.86	0.86-0.90
Cloud point (°C)	5	9	-1	Report
Pour Point (°C)	-10	-9	-5	Report
Viscosity (cSt)	6.30	6.51	4.78	1.9-6.0
Acid number	0.97	1.11	0.19	<0.5
FAME (GC)	51	45	98	>96.5
FAME (TG)	62.95	60.5	100	

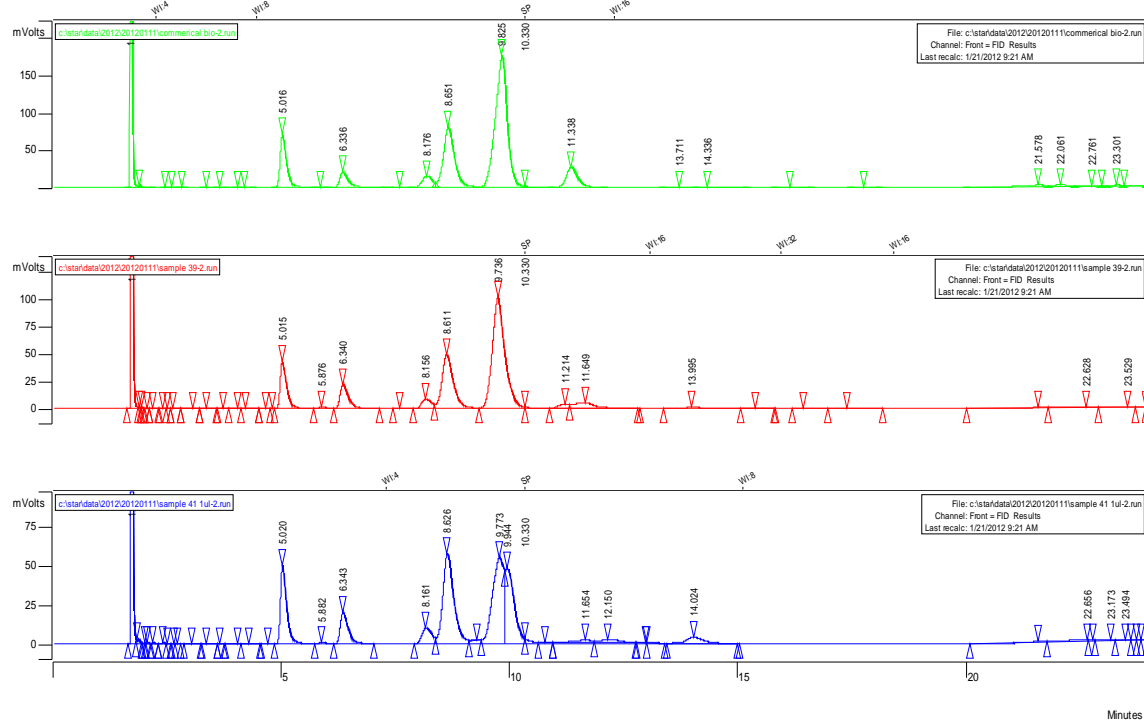
At the ambient pressure condition, methanol and bio-oil were not inter-soluble. Methanol, under the supercritical condition, seemly changed the solubility of bio-oil, thus greatly improve the conversion efficiency of bio-diesel. The supercritical methanol was confirmed to be good co-solvent. This could also explain why pressures close to the supercritical condition (about 250 C and 80 bar) was proper for improvement the conversion of the bio-diesel, which was not significant in improvement as pressures were continuously elevated.

The FAME contents in reaction products, reported by GC (the ASTM standard method), was slightly lower than those, reported by TG (our thermal analysis method). Two of the values for the same samples were within 10%, except for Sample 41 (about 14%). These results provide credence that our thermal analysis approach could be a quick reference method. Several critical parameters on the qualities of produced biodiesel were also presented in Table 21. Because of the incomplete conversion of the bio-oil, which was mixed with the produced biodiesel, samples 39 and 41 had similar densities, cloud points, pour points, and viscosities as compared to those of the commercially available biodiesel sample. However, these samples also had much higher acid numbers than the commercially available biodiesel sample. It is expected that further purification

Novel Oxygen Carriers for Coal-fueled Chemical Looping

of biodiesel products or promotion of the complete conversion of bio-oil could significantly decrease the acid number, as well as, increase other quality factors of the produced biodiesel. The GC analysis results are shown in Figure 27.

Figure 27. Overlay of sample 39, 41 and commercial biodiesel



Thermal analysis is a good technique for evaluating the characteristics of the biodiesel, such as thermal and oxidative stability, phase transitions and water absorbing ability. Moreover, in thermal analysis only a small amount of sample was needed compared with the standard analysis method. The thermal characteristics of the biodiesel was evaluated by using thermogravetric analyzer (TGA), differential scanning calorimetry (DSC), pressurized differential scanning calorimetry (PDSC), and sorption analyzer (SA). TGA results showed that the onset decomposition temperature and the peak temperature of the biodiesel was 193 and 225 °C in nitrogen flow respectively, indicating that the biodiesel has good thermal stability. The water content of the biodiesel was 0.1%. The oxidation onset temperature of the biodiesel was 152 °C and the oxidation induction time was 24 mins. DSC results showed that the onset crystallization temperature of the biodiesel was 1.0 °C. The preferable storage condition for the biodiesel occurs when the humidity is less than 30%.

Novel Oxygen Carriers for Coal-fueled Chemical Looping

Transesterification of Bio-oil Using Syngas and Methanol Catalysts

Previous both self-made and commercial heterogeneous catalysts have been tested and confirmed effectiveness on catalysis of the reaction of methanol transesterification of bio-oil to produce the bio-diesel. Considering the original function of the methanol synthesis catalyst, there is likelihood to direct biodiesel production through transesterification reaction from syngas, not from originally methanol.

Initially, three catalysts, which are in different shapes and particle sizes but same chemical formula, have been applied in the direct-syngas bio-oil transesterification tests under the ambient pressure and in a temperature range between 150 °C to 250 °C. The tests indicated the selected catalyst is functional on the conversion of the direct-syngas bio-oil transesterification. But the average conversion efficiencies under applied conditions were only 20 - 25%, as shown in Table 21. The smaller particle size of catalyst seemed to promote bio-oil conversion, but not significantly. Considering the occurrence of the higher pressure loss and even hard for operation if the fine particle catalyst was applied, the pelletized catalyst was applied to prevent larger pressure loss. There was an optimal temperature range for the promotion of the syngas-direct bio-oil transesterification, which was about 200 °C in the given syngas compositions. The increase of pressures significantly improve conversion efficiencies of transesterification, as indicated in Table 22.

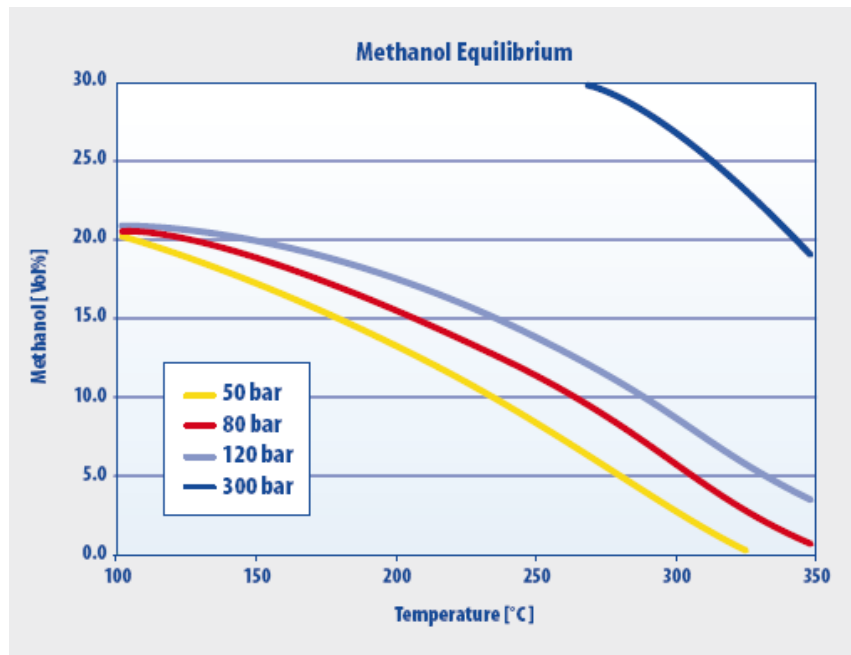
Table 22. Syngas-direct bio-oil transesterification

Temperature (C)	Pressure (bar)	Syngas Flowrate				Bio-oil flowrate (ml/min)	Catalyst	Bio-diesel conversion effic.
		N ₂	H ₂	CO	CO ₂			
160	1atm	x	1.2	0.6	0.2	0.1	Commercial Catalyst -fine particle	23.64
200	1atm	1.2	x	0.6	0.2	0.1	Commercial Catalyst -fine particle	25.61
200	1atm	1.2	x	0.6	0.2	0.1	Commercial Catalyst -fine particle	25.49
200	1atm	x	1.2	0.6	0.2	0.1	Commercial Catalyst -fine particle	25.81
200	1atm	x	1.2	0.6	0.2	0.1	Commercial Catalyst -self pelletization	24.89
250	1atm	x	1.2	0.6	0.2	0.1	Commercial Catalyst -self pelletization	18.65
250	1atm	x	1.2	0.6	0.2	0.1	Commercial Catalyst -self pelletization	17.14
250	1atm	x	1.2	0.6	0.2	0.01	Commercial Catalyst -self pelletization	19.95
200	1atm	x	1.2	0.6	0.2	0.01	Commercial Pelletized Catalyst	22.94
150	100	x	1.2	0.6	0.2	0.1	Commercial Catalyst -self pelletization	46.39
250	100	x	1.2	0.6	0.2	0.1	Commercial Catalyst -self pelletization	47.07
300	100	x	1.2	0.6	0.2	0.1	Commercial Catalyst -self pelletization	36.95

Novel Oxygen Carriers for Coal-fueled Chemical Looping

Figure 28 presented the equilibrium studies of maximization of methanol production under corresponding temperatures and pressures. It exhibits the necessarily to optimization of methanol production under higher pressures and temperatures. Higher pressures and lower temperatures regularly increase equilibrium conversion efficiencies of methanol synthesis. Previous practiced supercritical methanol under 80 bar and 250 °C seemed not optimal in the view of the equilibrium of methanol synthesis using syngas, when the best results of bio-oil conversion was obtained. To balance both reactions of the methanol synthesis and the followed bio-oil transesterification under supercritical condition, a new mechanism must be followed. In the integrated process, the synthesized methanol would be consumed in the followed-up bio-oil transesterification reaction, when the equilibrium of methanol synthesis would not ever been reached. The maximum methanol concentrations may not limit kinetics of the transesterification reaction.

Figure 28. Equilibrium conversion efficiency of methanol synthesis using syngas



Supercritical Transesterification Using Bio-oil and Cellulose Biomass

Direct integration of the cellulosic biomass into the feedstock stream is an even bold step to further improvement of direct bio-oil transesterification, compared to the direct bio-oil transesterification for bio-diesel production using syngas ($H_2 + CO$) and methanol synthesis

Novel Oxygen Carriers for Coal-fueled Chemical Looping

catalysts. Test results indicated that there was only a minimum production of methanol as well as bio-diesels if the biomass was directly to be feedstock. Further studies revealed the current bench-top stirring reactor system was partially responsible for a lower conversion efficiency of bio-diesel production directly using biomass, because it was not qualified for handling two reactions with different phases of feedstock (syngas in the gas phase, and bio-oil in the liquid phase). Another reason leading failure of direct-biomass bio-oil transesterification was the pyrolysis or decompositions of both biomass, which occurred under the elevated temperatures and pressures. Tests indicated that the complicated compounds have been generated under elevated pressures (to 280 bar) and temperatures (to 350 °C) if the cellulosic biomass was fed in with bio-oil. The reaction products have been identified as pyrolysis product of the cellulosic biomass, which was unavoidable when biomass was used as feedstock in our process. The mass balance calculation indicated that the conversion efficiencies of the pyrolyzed chars were lower under typical conditions of applied pressures and temperatures in this study (residence time varied between 1 hour to 3 hour). A further built continuous flow high pressure reactor seemed unable to handle feeding and reaction of solid feedstock of biomass. Because of all these reasons, our practices on using biomass as feedstock into bio-oil transesterification stopped.

5.4 Final Solution on Process Couplings

The process regarding the direct feeding of cellulosic biomass was confirmed to be infeasible, because an existing technical conflicts in optimal operational conditions between the syngas production using cellulosic biomass and transesterification of bio-oil. However, a modified process starting with a syngas feeding into the transesterification of bio-oil, which excluded the biomass gasification, was successfully accomplished for bio-diesel production. The catalyst used in this modified process was from a commercial supply, which was originally designed for production of methanol. A methanol catalyst was presented effective for transesterification of bio-oil. The optimal conditions for this new process were temperature dependent, not pressure dependent above the supercritical pressure of methanol, although a higher pressure was preferable for methanol synthesis in view of thermodynamics. This was because methanol was only an intermediate product, and thus was not required in a higher concentration which was limited by thermodynamics of the syngas-to-methanol reaction. Overall,

Novel Oxygen Carriers for Coal-fueled Chemical Looping

the gasification of cellulosic biomass should be excluded from the integrated process, and a gasification of biomass to produce syngas should be separately operated.

The accomplishment of the modified process was in its instant integration of commercially-available refinery process, which is cost effective for the bio-diesel production. The accomplishment was also extended to the confirmation of the effectiveness of commercial methanol catalysts on both the methanol synthesis and the followed-up methanol transesterification of bio-oil to produce the bio-diesel. Combining both of two unique accomplishments, cost reductions based on this new bio-refinery process, using available commercial facility to produce the bio-diesel, could be expected. The most likely commercial process which could be used for this process would be the inexpensive methanol synthesis facility and process.

This will potentially open a door for our technology combined into the current available refinery industries for cost-saving purpose. Previous tests also identified the initial idea to directly combine biomass cellulose into the biodiesel production is more challenging. Balancing all aspects of our current funding throughout this project so far, we determine to finally apply an approach starting from the synthesis gas to produce bio-diesel, which is more practical. The synthesis gas is produced from cellulose biomass through a separated process, because the exclusion of complexity of the cellulose biomass gasification out of the one-step strategies of biodiesel production will largely improve purity of synthesized biodiesel and simply the whole process. Most importantly, the new bio-diesel production process should be very similar to the methanol synthesis process. Thus, all equipment of the methanol synthesis, which have long been commercial available could be used to produce bio-diesel. This would be commercially mature for the economic-effective bio-refinery process.

6. Conclusion

A previously proposed process regarding the direct feeding of cellulosic biomass was confirmed to be infeasible for bio-diesel production, because an existing technical conflicts in optimal operational conditions between the syngas production using cellulosic biomass and transesterification of bio-oil. However, a modified process starting with a syngas feeding into the transesterification of bio-oil, which excluded the biomass gasification, was successfully accomplished for bio-diesel production. The catalyst used in this modified process was from a commercial supply, which was original for production of methanol. A methanol catalyst was presented effective for transesterification of bio-oil. The optimal conditions for this new process were temperature dependent, not pressure dependent, although a higher pressure was preferable for methanol synthesis in view of thermodynamics. This was because methanol was only an intermediate product, and thus was not required in a higher concentration which was limited by thermodynamics of the syngas-to-methanol reaction. Overall, the gasification of cellulosic biomass should be excluded from the previously proposed integrated process, and a separately operated gasification of biomass-derived syngas should be on line.

The accomplishment of the modified process was in its instant integration of commercially-available refinery process, which is cost effective for the bio-diesel production. The accomplishment was also extended to the confirmation of the effectiveness of commercial methanol catalysts on both the methanol synthesis and the followed-up methanol transesterification of bio-oil to produce the bio-diesel. Combining both of two unique accomplishments, cost reductions based on this new bio-refinery process, using available commercial facility to produce the bio-diesel, could be expected. The most likely commercial process which could be used for this process would be the inexpensive methanol synthesis facility and process.

7. Acknowledgement

Financial support for this project was provided by the U. S. Department of Energy National Energy Technology Laboratory (Cooperative Agreement NO. DE-EE0003156), and Kentucky Energy and Environmental Cabinet. Finally, the contributions of the project team members who actually executed the project work are greatly appreciated.

8. References

1. U.S. Department of Energy, Energy Information Administration. Basic Petroleum Statistics. www.eia.doe.gov/neic/quickfacts/quickoil.html. Accessed in July **2007**.
2. U.S. Department of Energy. Emissions of Greenhouse Gases in the United States **2005**. www.eia.doe.gov/oiaf/1605/flash/flash.html. Accessed in **2007**.
3. Hoffert, M. I.; Caldeira, K.; Jain, A. K.; Haites, E. F.; Harvey, L. D. D.; Potter, S. D.; Schlesinger, M. E.; Schneider, S. H.; Watts, R. G.; Wigley, T. M.L.; Wuebbles, D. J. *Nature*, **1998**, 395:881.
4. BP, Statistical Review of World Energy **2007**. www.bp.com/productlanding.do?categoryId_6842&contentId_7021390. Accessed in August, **2006**.
5. Hirsch, R. L.; Bezdek, R.; Wendling, R. **2006**, *AIChE J.* 52:2.
6. National Research Council (**2004**) The Hydrogen Economy: Opportunities, Costs, Barriers, and R&D Needs. Natl. Acad. Press, Washington, DC. Accessed in **2007**.
7. MacLean, H. L.; Lave, L. B. *Progr. Energ. Combust. Sci.*, **2003**, 29:1.
8. Tarascon, J. M; Armand, M. *Nature*, **2001**, 414:359.
9. Interagency Agricultural Projections Committee. USDA Agricultural Baseline Projections to 2015 (Dept. of Agriculture, Washington, DC), DOE Publ. No. OCE-2006-1.
10. U.S. Department of Energy, Energy Information Administration. Annual Energy Outlook 2006 with Projections to 2030 (Dept. of Energy, Washington, DC), DOE Publ. No. EIA-0383 (**2006**).
11. Fargione, J.; and et al. *Science*, **2008**, February 29, 1235.
12. Searchinger, T.; and et al. *Science*, **2008**, February 29, 1238.
13. James, T.; and Timothy, D. Microbes in the Energy Grid. *Science*, **2008**, May 23, 985
14. Stephen, K. R. On the Road to Green Gasoline. *Chemical&Engineering News*, American Chemistry Society, **2008**, November 27, 57-59
15. Hill, J.; Nelson, E.; Tilman, D.; Polasky, S.; Tiffany, D. *PNAS*, **2006**, 103(30):11206.
16. Hess, G. *Chemical & Engineering News (ACS)*, **2007**, 85(41): 35.
17. GOVERNOR STEVEN L. BESHEAR. Intelligent Energy Choices for Kentucky's Future - Kentucky's 7-Point Strategy for Energy Independence, November **2008**.
18. Guidelines for KREC Competitive Grants Program **2009** Request for Proposals. The Kentucky Renewable Energy Consortium, Administered by KPPC – Kentucky Pollution Prevention Center, www.kppc.org/KREC, **2009**.
19. Demirbas, A. *Energy Conversion & Management*, **2006**, 47: 2271.
20. Marchetti, J. M.; Miguel, V. U.; Errazu, A. F. *Renewable & Sustainable Energy Reviews*, **2007**, 11:1300.
21. Karaosmanoglu, F; Cigizoglu, K. B.; Tuter, M.; Ertekin, S. *Energy&Fuel*, **1996**; 10:890.
22. Freedman, B.; Pryde, E.H.; Mounts, T.L. *J. Am. Oil Chem. Soc.* **1984**, 61:1638.
23. Komers, K.; Macheck, J.; Stloukal, R. *Eur. J. Lipid Sci. Technol.*, **2001**, 103, 359.
24. Ma, F.; Clements, L.D.; Hanna, M.A. *Trans. ASAE*, **1998**, 41:1261.
25. Demirbas, A. *Energy Sources*, **2002**, 24:835.
26. Kusdiana, D.; Saka, S. *Fuel*, **2001**, 80:693.
27. Saka, S.; Kusdiana, D. *Fuel* **2001**, 80:225.
28. Bala B.K. *Energy Edu. Sci. Technol.* **2005**, 15:1–45.
29. Krammer, P.; Vogel, H. *Supercritical Fluids*, **2000**, 16:189.

Novel Oxygen Carriers for Coal-fueled Chemical Looping

30. Balat, M. *Energy Edu. Sci. Technol.*, **2005**, 16:45.
31. Demirbas, A. *Progress Energy Combus Sci.*, **2005**, 31:466.
32. Marchetti, J. M.; Errazu, A. F. Technoeconomic Study of Supercritical Biodiesel Production Plant. *Energy Conversion and Management*, **2008**, 49, 2160.
33. Jean-Paul Lange. *Catalysis Today*, **2001**, 64: 3.
34. Dijk, C. V.; Fraley, L. D. *WO Patent 91/15446*, **1991**, Starchem.
35. Westerterp, K.R. in: Proceedings of the European Applied Research Conference on Natural Gas Eurogas '92, Trondheim, Norway, **1992**, p. A35.
36. Dandekar, H. W. Funk, G. A. *US Patent 5,449,696*, **1996**, UOP.
37. Struis, R. P. W.; Stucki, S.; Wiedorn, M. J. *Membr. Sci.* **1996**, 113:93.
38. Westerterp, K. R.; Bodewes, T. N.; Vrijland, M. S. A.; Kuczynski, M. *Hydrocarbon Process*, **1988**, 67 (11): 69.
39. Berty, J. M.; Krishnan, C.; Elliott Jr., J. R. *Chemtech*, **1990**, 20: 624.
40. Schneider III, R. V.; LeBlanc Jr., J. R. *Hydrocarbon Process*. **1992**, 71(3): 51.
41. Lange, J.-P. *Ind. Eng. Chem. Res.* **1997**, 36: 4282.
42. Guo, Y. S.; Zhong, J.; Xing, Y.; Li, D.; Lin, R. *Energy&Fuel* **2007**, 21: 1188.
43. Cao, Y.; Pan, W. P. *Energy Fuels*, **2008**, 22 (3), 1720–1730.
44. Olah, G. A.; Goeppert, A.; Surya Prakash, G. K. *Beyond Oil and Gas: The Methanol Economy*. 2006 WILEY-VCH Verlag GmbH & Co. KgaA, Weinheim, ISBN 3-527-31275-7
45. Castello, M.L.; Dweck, J.; Aranda, D.A.G. *J. Therm Anal Clorim*, **2009**: 97: 627-630.
46. Conceicao, M.M.; Fernandes, V.J.; Araujo, A.S.; Farias, M.F.; Santos, I.M.G.; Souza, A.G. *Energy & Fuels*, **2007**, 21: 1522-1527.
47. Candeia, R.A.; Sinfronio, S.M.; Bicudo, T.C.; Queiroz, N.; Barros, Filho K.D, Soledade, L.E.; Santos, I.M.G.; Souza, A.L. *J. Therm Anal Calorim*. DOI 10.1007/s10973-011-1287-1.
48. Xu, B.; Xiao, G.M.; Cui, L.F.; Wei, R.P.; Gao, L.J. *Energy & Fuel*, **2007**, 21: 3109-3112.
49. Rodriguez, R.P.; Sierens R.; Vehelst, S. *J. Therm. Anal. Claorim*. 2009, 96: 897-901.
50. Teixeira, G.A.A.; Maia, A.S.; Santos, I.M.G.; Souza, A.L.; Souza, A.G.; Queiroz, N. J. *Therm. Anal. Calorim*. DOI 10.1007/S10973-011-1626-2.
51. Robertis, E.D.; Moreira, G.F.; Silva, R.A.; Achete, C.A. *J Therm Anal Calorim*, DOI 10.1007/s10973-011-1571-0.
52. ASTM D 6571: Standard Specification for Biodiesel Fuel Blend Stock (B100) for Middle Distillate fuel, **2008**.
53. Sharma, Y.C.; Singh B.; Upadhyay S.N. Advancements in development and characterization of biodiesel: A review. *Fuel*, **2008**, 87: 2355-2373.
54. Korres D.M.; Karonis D.; Lois E. Aviation fuel JP-5 and biodiesel on a diesel engine. *Fuel*, 2008, 87: 70-78.ion for Biodiesel Fuel Blend Stock (B100) for Middle Distillate fuel, 2008.
55. O'Connor CT, Forrester RD, Scurrell MS. *Fuel*, **1992**, 71: 1323-1327.
56. Chand, P.; Chintareddy, V.R.; Verkade, J.G.; Grewell, D. *Energy & Fuels*, **2010**, 24: 2010-2015.
57. Thomas Hielscher. Ultrasonic production of nano-size dispersions and emulsions. ENS' 05, Paris, France, **2005**, 14-16.
58. Singh, A.K.S.; Fernando, S.D.; Hernandez, R. *Energy & Fuels*, **2007**, 21: 1161-1164.
59. Georgogianni, K.G.; Kontominas, M.G.; Pomonis, P.J.; Avlonitis, D.; Gergis, V. *Energy & fuels*, **2008**, 22: 2110-2115.
60. Zabeti, M.; Wandaud, W.M.A.; Aroua, M.K.; *Fuel Processing Technology*, **2009**, 90: 770-777.

Novel Oxygen Carriers for Coal-fueled Chemical Looping

61. Refaat, A.A. *Journal of Environmental Sience & Technology*, **2011**, 8(1): 203-211.
62. Abreu, F.R.; Lima, D.G.; Hamu, E.H.; Einloft, S. Rubim, J.C.; Suarez, P.A.Z. New metal catalysts for soybean oil transesterification. *Journal of the American Oil Chemists' Society*, **2003**, 80: 601-604.
63. Mahamuni, N.N.; Adewuyi, Y.G. *Energy Fuels*, **2010**, 24: 2120-2126.
64. Silva, C.C.; Ribeiro, N.F.P.; Souza, M.M.; Aranda, D.A.G. *Fuel Processing Technology*, **2010**, 91: 205-210.
65. Wen, L.B.; Wang, Y.; Lu, D.L.; Hu, S.Y.; Han, H.Y. *Fuel*, **2010**, 89: 2267-2271.

66. Demirbas, A.; *Energy Sources*, **2002**, 24:835.
67. Kusdiana, D.; Saka, S. *Fuel*, **2001**, 80:693.
68. Saka, S.; Kusdiana, D. *Fuel* **2001**, 80:225.
69. Bala BK. Studies on biodiesels from transformation of vegetable oils for Diesel engines. *Energy Edu Sci Technol* **2005**, 15:1-45.
70. Krammer, P.; Vogel, H. *Supercritical Fluids*, **2000**, 16:189.
71. Balat, M. *Energy Edu. Sci. Technol.*, 2005, 16:45.
72. Demirbas, A. *Progress Energy Combus Sci*, **2005**, 31:466.
73. Jean-Paul Lange. *Catalysis Today*, **2001**, 64: 3.